This is to certify that the

thesis entitled

A Kinetic Study of the Role of Oxygen in
Hydrogasification of Saran Char and Coal Char

presented by

Michael Gerard Lussier Jr.

has been accepted towards fulfillment
of the requirements for

M.S. degree in Chem. Engr.

Dennis J. Miller
Major professor

Date 3/18/92

A KINETIC STUDY OF THE ROLE OF OXYGEN IN HYDROGASIFICATION OF SARAN CHAR AND COAL CHAR

By

Michael Gerard Lussier Jr.

A THESIS

Submitted to
Michigan State University
in partial fulfillment of the requirements
for the degree of

MASTER OF SCIENCE

Department of Chemical Engineering

1992

693-3221

ABSTRACT

A KINETIC STUDY OF THE ROLE OF OXYGEN IN HYDROGASIFICATION OF SARAN CHAR AND COAL CHAR

By

Michael Gerard Lussier Jr.

The effect of several sample treatments on the hydrogasification rate of an Illinois'6 coal char and Saran char were investigated. Uncatalyzed rates at 725°C and 3.3MPa H_2 decayed rapidly with conversion for both chars. Hydrogen pretreatment was shown not to affect rate, and rate was shown not to correlate well to total surface area within the first 15-25% carbon conversion. Outgassing was shown to decrease the reaction rate, due to annealing, by an order of magnitude. Partial combustion in air was used to fix oxygen functional groups on char surfaces. Oxidation of fresh chars did not measurably increase hydrogasification rates at 725°C, but oxidation of outgassed chars or chars previously reacted with hydrogen increased rate by a factor of two to three. Potassium carbonate catalyzed hydrogasification of all chars, but was poisoned by coal ash. Three separate reaction stages during hydrogasification have been proposed based on the findings in this investigation.

I dedicate my masters thesis to my parents Michael and Roseann Lussier, and my sister Amy Lussier.

ACKNOWLEDGEMENTS

I would like to thank Dr. Dennis J. Miller, my graduate advisor, for his strong support and guidance during the course of my Masters research and thesis work. Thanks must also go to Dr. Martin C. Hawley and Dr. Lawrence T. Drzal for accepting the task of serving on my committee.

I would like to thank Captain Martin E. Toomajian for the hard work put into sample analysis, as well as Mark Benedict.

Finally, I would like to thank the United States Department of Energy for their financial support through grant #DE-FG22-89PC89777.

TABLE OF CONTENTS

LIST OF TABLES

LIST OF FIGURES

CHAPTER 1

INTRODUCTION

1.1. BACKGROUND

Coal hydrogasification is the conversion of coal to methane via reaction with hydrogen at elevated temperatures and pressures, causing complete enrichment of carbon with hydrogen. There are many reasons why coal hydrogasification is beneficial. Synthetic natural gas is a much cleaner burning fuel than coal, and is capable of being transported by pipeline. The current world supply of natural gas is not a renewable resource, and is rapidly being depleted. Even though coal is also a nonrenewable resource, conversion of it to natural gas may bridge the time lag between depletion of natural gas and the development of alternative energy sources such as nuclear, solar, and biological.

Steam gasification has been studied most extensively and has been used commercially to convert coal to natural gas. It does not require pressures as high as hydrogasification, does not have a rate that declines rapidly with conversion, and is not equilibrium limited at higher temperatures as is hydrogasification. The main reactions that take place during steam gasification are as follows:

a] $C + H_2O \longrightarrow H_2 + CO$ synthesis gas formation

b] $CO + 3(H_2) \longrightarrow CH_4 + H_2O$ methanation

c] $CO + H_2O \longrightarrow H_2 + CO_2$ water shift reaction

The study of hydrogen gasification does have distinct advantages over steam gasification, despite the fact that it requires higher pressures and is limited by equilibrium conditions at higher temperatures. The basic reaction that takes place during hydrogasification is as follows:

d] $C + 2H_2 \longrightarrow CH_4$

Hydrogasification is a direct exothermic method of methane production. Unlike reactions occurring in steam gasification, it is strictly a surface reaction.

The reaction rate during hydrogasification declines rapidly with conversion. This is a disadvantage from a process perspective, but can lend a great deal of insight to questions about rate kinetics and mechanisms.

Hydrogasification rate can be increased by addition of a number of catalysts, including alkali and alkali earth metals and salts, as well as transition metals. Oxygen functional groups on the coal surface are thought to play a key role in methane formation. The only oxygen present during hydrogasification is that which is already associated with the solid, so it can be studied closely.

Hydrogasification is an important step in several coal conversion processes. It is the primary reaction in the HYDROCARB process, which is a method of producing very high purity carbon from a variety of coals, wastes, and biomass materials.[1] It may be a significant means of increasing methane yields in the Exxon gasification process,[2] and is the primary route to methane formation in systems that possess significant partial pressures of hydrogen.[3] Even though hydrogen is currently too valuable a commodity to be used in large-scale methane production, it may be the best route if an abundant hydrogen source is developed.

1.2. LITERATURE REVIEW

1.2.1. UNCATALYZED HYDROGASIFICATION

1.2.1.1. GENERAL REACTION PHENOMENA

Much of the pioneering work on coal hydrogasification was done by J.D. Blackwood et al. They were able to determine that reaction rate is proportional to hydrogen partial pressure during initial stages of carbon conversion,[4-7] and that rate is not a strong function of char type.[4,8,9] Other researchers also determined that methane formation rate is first order in hydrogen partial pressure.[10] The uncatalyzed hydrogasification rate decreases rapidly with carbon conversion,[5,7,11-14] which led some researchers to claim that the initial rate is diffusion controlled.[15] Activation energies reported include values of 43 kcal/mol[4] and 27 kcal/mol,[10] but the extent of carbon conversion where the rate data were taken is not specified. Other researchers reported activation energies of 36 kcal/mol initially to 51 kcal/mol at steady state,[15] and 15 kcal/mol initially to 50 kcal/mol at steady state.[16] Activation energies of the cleavage of carbon-carbon bonds in steam and carbon dioxide char gasification include values of 80.5 kcal/mol [17] and 61.4 kcal/mol [18] respectively.

Almost all chars possess a high internal surface area resulting from a complex pore network. The char base structure can be thought of as a collection of small randomly aligned graphite crystallites.[19] Porosity and thus surface area is the result of poor crystallite packing due to random alignment. Total char surface area as determined by BET analysis, however, correlates very weakly or does not correlate at all with gasification rate. This has been shown for oxygen gasification,[20] carbon dioxide gasification,[21,22] as well as hydrogasification.[9,23] In the case of oxygen gasification, developing pores include those in the micro- and mesopore range, which restrict molecular diffusion.[20] In the case of hydrogasification, macropore surface area does not increase until about 55% carbon conversion. Widening of the micro- and mesopores is the main reason for the increase.[24]

Structure on the molecular level appears to be much more important in determining hydrogasification rate. Several two-stage reactions have been proposed by researchers to explain the rapid rate decay in hydrogasification. One claim is that the initial high rate results from reaction of hydrogen with amorphous carbon atoms which were deposited during pyrolysis.[8] Prior to pyrolysis, most of the char internal volume is filled with compounds that are volatile relative to the char base structure. During pyrolysis, some of these compounds completely volatilize, and some carbonize. The carbonized char coats part of the char surface in an amorphous form. This amorphous, or "secondary carbon," tends to be more saturated with hydrogen and less saturated with chemical bonds in general. The low steady state rate is due to reaction of hydrogen with the graphite-like char base structure.[8] The same researchers have proposed a similar model in which initial high reaction rate results from gasification of carbons associated with oxygen functional groups.[25] Other researchers used unpyrolyzed chars and make the claim that high initial rate is due to pyrolysis of aliphatic side chains and oxygenated functional groups followed by hydrogenation of intermediate pyrolysis products. The low steady state rate is due to direct attack of residual aromatic base char structures.[26]

A strong preference for reaction of hydrogen with edge carbon atoms, as opposed to basal plane carbon atoms, has also been shown.[27] This is because of unpaired sigma electrons on edge carbon atoms which make them more reactive than those of the basal plane. It may also result in part from diffusion of impurities which serve as catalysts or leave vacancies if they desorb from edge carbons.[28] Further probing into the reactivity of edge carbon atoms by etch pit analysis of graphite shows that hydrogen greatly prefers to attack the "armchair" edge carbons ($<112l>$ edge plane) over the "zig-zag" edge carbons ($<101l>$ edge plane) in hydrogasification and steam gasification,[29-32] while oxygen and carbon dioxide show no edge preference in gasification.[29,32] Etch pits formed during hydrogasification and steam gasification were hexagonal, oriented such that all edges were composed of zig-zag configurations. Etch pits formed during oxygen and carbon dioxide gasification were round, indicating both configurations on the pit edge. Although coal is not graphite, it is highly aromatic, and can be assumed graphitic on a local level.[19] Various edge and pit configurations are illustrated in Figure 1.

Understanding the way in which hydrogen adsorbs onto the char surface is also an important part of determining what takes place during reaction. Several researchers have suggested successive dissociative hydrogen chemisorption onto adjacent carbon atoms.[16,33] Some have gone further and suggested that the breakage of the bond between adjacent carbons, which is caused by the adsorption of the third pair of hydrogen atoms, is the rate limiting step.[30] Associative hydrogen chemisorption has also been suggested as a possible methanation mechanism. Two hydrogen molecules successively adsorb onto the same carbon atom, completely enriching it.[34] It has also been suggested that

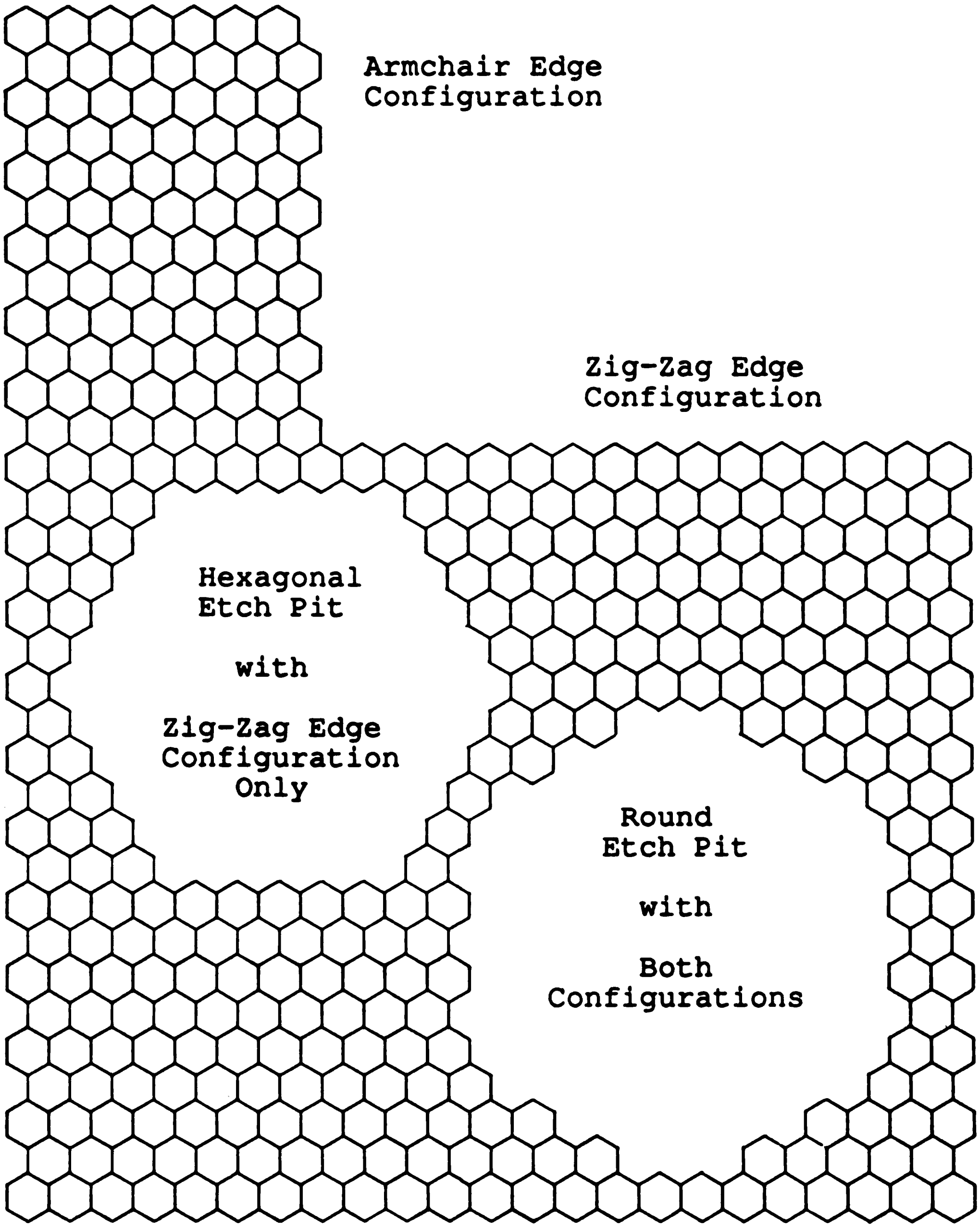

Figure 1: Various Edge Configurations on the Graphite Basal Plane

dissociative hydrogen chemisorption occurs first followed by associative chemisorption, with the dissociative step being rate limiting.[6]

Understanding the role of hydrogen in gasification of chars is also important because it has been shown to inhibit steam and carbon dioxide gasification.[35-41] It may also be part of the cause of rapid deactivation of hydrogasification rate due to dissociative adsorption [42].

With the idea of associative hydrogen chemisorption, these researchers have also introduced the concept of an active site.[6] It is generally defined as a carbon atom on the char surface that is not completely saturated with chemical bonds, or a carbon with free or unpaired electrons.[9] An active site is where hydrogen associatively adsorbs, and when the carbon is saturated with hydrogen and cleaved from the char surface another active site is be generated on an adjacent carbon.

1.2.1.2. ROLE OF OXYGEN

It is generally believed that the major source of active sites in all gasification reactions comes from the desorption of oxygen functional group from the char surface. These groups desorb in the form of carbon monoxide and carbon dioxide when samples are heated to reaction temperature,[7,43-50] and in the form of water during reaction.[7] The desorption of carbon monoxide and carbon dioxide is considered the rate limiting step in oxygen gasification,[51] and determines the rate of this reaction.[23] Hydrogasification rate has been shown to be a strong function of the oxygen content of various chars,[4,7,52] and initial rate a strong function of oxygen surface concentration.[48,53] It has also been shown to be a strong function of char preparation temperature,[4,8,9,54] because char oxygen content is a strong function of preparation temperature.[4,7]

There are several methods of fixing oxygen onto char surfaces in an attempt to increase the active surface area, and therefore the gasification rate.[46,47] One method is partial combustion in oxygen before carbon dioxide gasification [55,56] and hydrogasification.[48-50,57,58] Chemical methods include treatment with nitric acid,[48,59,60] peracetic acid,[61] or hydrogen peroxide.[62] Continuous oxidation can be performed by addition of low concentrations of oxygen or carbon dioxide to the reactant gas in hydrogasification.[63]

The most widely used general description of oxygen functional groups on char surfaces is the pH of these sites, which is determined by their formation conditions.[64] Groups generally thought of as acidic include carboxyl and phenolic hydroxyl groups [64][65] and lactone groups.[66-69] Acidic groups are formed during partial combustion in oxygen at temperatures ranging from 300°C to 450°C,[70] or to 500°C.[70-73] Some researchers have claimed that the optimum oxidation temperature is 400°C.[72,74] Acidic groups generally desorb as carbon dioxide during sample heatup.[70] Nitric acid treatments generally fix acidic functional groups onto char surfaces,[50] but basic groups can be fixed as well.[62,75] Among the groups fixed by nitric acid are carboxyl, phenol, amine, carbonyl, and ester groups.[76] Hydrogen peroxide can also form a mixture of functional groups.[62,75] Groups generally thought of as basic include pyrone-like structures and chromenes,[65,68] while neutral groups include carbonyls.[71] Basic groups are formed during partial combustion in oxygen at temperatures ranging from 700°C to 800°C,[62] or at 750°C +.[77,78] Basic and neutral groups generally desorb as carbon monoxide during sample heatup.[65,71] It is possible that the chromine groups, which oxidize to lactone groups,[68] may cause the low char reactivity during the later stages of sample conversion during hydrogasification up to temperatures of 870°C.[66]

Char reactivity can be decreased by heating samples to temperatures near 1000°C. This has been shown to greatly anneal char surfaces,[79] and decrease active surface area.[80] Outgassing, which involves heating chars to high temperatures under vacuum, cleans carbon black of all acidic functional groups.[58] It has also been shown to decrease hydrogasification rates by a factor of six and reduce surface oxygen concentrations to nearly zero.[57]

1.2.2. CATALYZED GASIFICATION

There are a number of catalysts that can be used for increasing the gasification rate of chars. Catalysts include alkali carbonates and most of the transition metals in groups IIIB-VIIIB. Transition metal catalysts are more effective than alkali carbonates,[81-84] but they are also much more expensive.[37,85,86] Examples of transition metals used include nickel and iron,[87-89] copper,[90] and platinum.[91,92]

Potassium appears to be the best choice among the alkali metals. Rubidium and cesium are more active than potassium, but are very expensive. Sodium is cheaper than potassium, but the greater catalytic activity of potassium more than compensates for this.[93] The advantage of potassium over alkali earths such as calcium is the fact that potassium will evenly disperse itself over the char surface due to its high mobility, while calcium must be atomically dispersed to create comparable activity.[94]

Several mechanisms have been proposed for potassium carbonate catalysis of steam and carbon dioxide gasification. A number of researchers have suggested a redox cycle with decomposition and reformation of the carbonate[40,41,95-98]. Intermediates of alkali hydroxide in steam gasification, and alkali oxide in carbon dioxide gasification are included. Other researchers have proposed that an alkali metal non-stoichiometric oxide serves as a center for the capture of oxygen from the gas phase and electrons from the char, which greatly increases the reaction of adsorbed oxygen atoms.[99-101] Potassium hydroxide has been suggested as an intermediate during this mechanism.[40] Another mechanism involving potassium-intercalation compounds has been proposed.[102]

Further research in this area has indicated that surface oxygen is essential for catalyst activity,[3] and is therefore involved in the mechanism.[52,53,103] Some researchers have claimed that the potassium to carbon ratio is what determines gasification rate,[103] but others have shown that the surface oxygen concentration is what determines the amount of retained potassium on the char.[52] The proposal of C-O-K complexes determining gasification rates has been supported by many researchers.[104,105] These complexes have been shown to be stable to 700°C and directly proportional to steam gasification rate.[39] A redox cycle has been proposed that involves the complex.[106] A possible mechanism for carbon dioxide gasification that includes the C-O-K complex consists of an alteration of the active catalyst between the complex and potassium metal. Carbon and oxygen are exchanged with the gas phase.[107]

Much less research has been done in the area of potassium carbonate catalysis in char hydrogasification. Significant rate enhancements have been observed,[58,108,109] but application of the above proposed mechanisms to catalyzed hydrogasification is limited because the oxidizing reactant gases, which support redox cycles, are not present.[93] A mechanism has been proposed which includes formation of the C-O-K complex by interaction between the catalyst and some basic surface groups.[58]

Another obstacle that must be overcome in catalyzed hydrogasification of coal chars is the strong inhibition caused by mineral matter in the ash. Catalyst poisoning with small amounts of sulfur has been observed during hydrogasification using potassium, as well as transition metals.[110] Aluminosilicates, mostly in the form of the clay minerals illite and kaolinite, poison potassium catalyzed steam gasification.[111,112]

1.3. PREVIOUS RESEARCH

Prior work by others in this research group focused on the role of oxygen in hydrogasification of uncatalyzed and potassium carbonate catalyzed chars. Zoheidi and Miller [50,58] concluded thermal decomposition of oxygen surface groups into CO and CO_2 leaves "nascent" active sites, therefore enhancing char reactivity with hydrogen. They observed rate enhancements with preoxidation of carbon black by oxygen chemisorption. Oxidation at 400°C produced mainly acidic groups which increased the initial rate about 100%, while oxidation at 800°C produced mainly basic groups which resulted in only minor rate enhancements. They also concluded stable rate enhancing complexes, which probably take the form C-O-K, are formed by the interaction of basic surface functional groups with the catalyst.

Treptau and Miller [48] showed by XPS analysis the surface oxygen concentration during uncatalyzed hydrogasification of carbon black and coconut char is essentially zero, and correlated initial rate to surface oxygen concentration. They observed uncatalyzed rate enhancements of about 70% with oxidation by HNO_3 pretreatment of carbon black, and 50% with HNO_3 preoxidation of coconut char. They also concluded basic surface functional groups interact with the potassium carbonate catalyst during hydrogasification to form stable rate enhancing complexes, which may take the form C-O-K.

1.4. RESEARCH OBJECTIVES

The coal hydrogasification reaction is very complex, and not well understood. It is known that steam and carbon dioxide gasification rates do not decay abruptly with conversion, like the rates in hydrogasification. The major objective of this research is to gain a more fundamental understanding of the reaction, and enhance the rate based on this knowledge. This focus of this research is the study of the role of oxygen in hydrogasification of coal, the investigation of the reaction inhibition by hydrogen, and the poisoning of the reaction by coal ash.

CHAPTER 2

EXPERIMENTAL

2.1. STARTING MATERIALS

The starting materials used in this investigation include a Dow Saran (R) MA 127 Resin and an Illinois #6 PSOC-1493 HVC Rank Coal. The Saran has been chosen as a model compound because it chars to a relatively pure carbon with an extremely low ash content and displays reactive and structural properties very similar to the coal chosen for this investigation. The coal has been selected because it is very well characterized and been widely used in other studies.

2.2. PYROLYSIS AND OXIDATION

2.2.1. QUARTZ TUBE REACTOR SPECIFICATIONS

The quartz tube reactor was used for pyrolysis of starting materials and low pressure oxidative treatments. It consists of a 4.8 cm ID quartz tube placed in a 1400 watt Lindberg Electric Furnace (Model 54232). The tube is 91 cm in length with a 0.6 cm nipple on the upstream end and a removable flange on the downstream end. Temperature is controlled with an Omega Series CN-2010 Programmable Temperature Controller. Firebrick plugs inside the quartz tube at both ends help minimize heat loss. Gases used in sample preparation include AGA 99.99% Nitrogen which passed through an Airco Single Stage Argon-Nitrogen-Helium Regulator for pressure control, and AGA Compressed Air U.S.P. which passed through a Rego Single Stage Regulator for pressure control. Gas flow rate was controlled by two rotameters in series. For high flow rate purging a 2-S-150 Fisher Scientific Laboratory Flow Meter was used, while for tightly controlled flow rates a Cole Parmer Model G Rotameter with a 420 cc/min maximum flow rate was used. Exhaust gas was sent through two water-filled 1000 ml Erlemeyer side-arm flasks in series to trap potentially hazardous products, then into a laboratory fume hood. The samples were placed in Coors U.S.A. Alumina Chemical-

Porcelain Ware Ceramic trays (4.0cm x 3.0cm x 0.5cm) or boats (10.4cm x 2.5cm x 1.5cm) during the reactions and were stored under nitrogen in capped glass bottles inside a desiccator.

2.2.2. PYROLYSIS

All starting materials were pyrolyzed because gasification of char is the rate limiting step in the overall gasification of coal. Charring rids starting materials of volatile components that may interfere with gasification. Saran was pyrolyzed mainly to expel chlorine and to enrich the carbon content of the sample. Coal was pyrolyzed mainly to expel tar-like hydrocarbons which can clog reactor lines, and to rid the sample of some sulfur which can poison the reaction, especially in the presence of catalysts. Ultimate analyses of Saran char and coal char are given in Table 2.1.

Samples were pyrolyzed by heating from 25°C to 900°C at 10°C/min, soaking at 900°C for 30 minutes, and cooling from 900°C to 100°C at 10°C/min. The actual cooling time was several hours because of the heavy insulation and large thermal mass of the furnace. Nitrogen flow rate was kept constant at 400 cc/minute and atmospheric pressure throughout all runs. With a reactor volume of 1650 cc, purge rate was about one reactor volume every four

Table 2.1: ULTIMATE ANALYSIS OF VARIOUS CHARS[116]

(Weight % on Dry Basis)

Element	Saran Char	Coal Char	Demin. I Char	Demin.II Char
% Carbon	96.36	75.30	88.59	92.00
% Hydrogen	0.53	0.53	0.69	0.39
% Nitrogen	1.04	1.34	1.40	3.50
% Sulfur	0.43	3.55	2.32	1.21
% Ash	0.08	17.33[1]	0.66[2]	1.36
% Oxygen (diff)	1.56	1.95	6.34	1.54
	100.00	100.00	100.00	100.00
% Chlorine			0.25	
Fluorine μg/g			163	
BTU/lb	14073	11300	12847	13471

1. Correct dry ash content is 20.81% because 3.48% sulfur is retained in the ash.

2. Correct dry ash content is 2.94% because 2.28% sulfur is retained in the ash.

minutes. An average of 51 grams of coal per run was loaded into the quartz tube reactor, with a yield of 61% +1%. An average of 12 grams of Saran powder was loaded per run with an average yield of 25.5% +0.5%. The Saran forms a greatly expanded foam-like structure of carbon when charred, which must be ground into a powder before use.

2.2.3. PARTIAL OXIDATION

Oxygen functional groups on char surfaces have an effect on char reaction rates. One of the main objectives of this investigation is to study this effect, so partial combustion in air was used as the main method of oxidizing char surfaces. All oxidations were performed in the quartz tube reactor using slightly different methods to achieve varying degrees of oxidation. The soak temperature used for most chars was 375°C, while 725°C was used in a few runs. Chars were held at the soak temperature for 0.5-3 hours and were subject to various combinations of air and nitrogen flow rates, or stagnant conditions, depending upon the desired conversion and the amount of char to be treated. Sacrificial carbon was used in some cases so not all of the oxygen will react with the sample of interest. Oxidation was used as a pretreatment or an intermittent treatment for some hydrogasifications.

2.2.3.1. PRETREATMENT

One procedure has been used for oxidative pretreatment of most chars. Five of the 0.5 cm deep ceramic trays were loaded into the quartz tube reactor, each containing 0.5 gram of Saran char or 1.0 gram of coal char. The reactor was heated from 25°C to 375°C at a rate of 10°C/min and held at 375°C for a designated time period. The reactor was purged with air at a flowrate of 50 cc/min during the heat ramp and soak, and then 250 cc/min of nitrogen during the time it took the reactor to cool down to room temperature, which was usually overnight. One batch of char was oxidized at 725°C, but the air was kept stagnant to prevent excessive conversion of the char. Shallow trays and small amounts of char were used to avoid large oxidation gradients within individual trays that would be caused by mass transfer limitations. Some conversion gradients were caused between trays because of the parabolic temperature profile within the heated zone of the reactor.

2.2.3.2. INTERMITTENT TREATMENT

The air flow rate for most intermittently oxidized samples was kept stagnant because the total mass of these samples was much less than that of the preoxidized chars.

Intermittently oxidized samples had weights less than 0.3 gram in the case of Saran char and 1.0 grams in the case of coal char, compared to 2.5 grams of Saran char and 5.0 grams of coal char for oxidative pretreatments. Two to three grams of sacrificial char were included in the reactor with most intermittent oxidations to prevent excessive sample conversion during oxidation.

2.3. DEMINERALIZATION

Some of the coal samples in this study were demineralized in order to study the effect of ash on both uncatalyzed and catalyzed coal char hydrogasification. Two methods of demineralization were used on the starting materials.

2.3.1. METHOD I

The first method was based on one taken from a paper on determination of coal mineral matter by Bishop and Ward,[114] and has been designated as Demineralization Method I. It included a hydrofluoric acid bath and a hydrochloric acid bath of previously pyrolyzed coal. Eighty grams of coal was mixed with 500 ml of a 49% hydrofluoric acid solution at 60°C for 1 hour while being stirred every 5 minutes. The slurry was vacuum filtered, then the filter cake was combined with 1000 ml of a 37% hydrochloric acid solution under the same conditions. The new slurry was then vacuum filtered, washed with 5 L of distilled water, and left overnight in 2000 ml of distilled water under constant agitation. The next day it was vacuum filtered, washed with 5 L of distilled water, and dried at 110°C under nitrogen overnight. On the third day it was pyrolyzed for a second time. This method did not work well for the coal used in this set of experiments. This may be due to ash particle encapsulation during initial pyrolysis and/or pyrites that resist both hydrofluoric and hydrochloric acids. An ultimate analysis of Demineralization Method I coal char is in Table 2.1.

2.3.2. METHOD II

The second method was developed to achieve a more complete demineralization than the first, and has been designated as Demineralization Method II. It contains most of the steps found in the first method, and also includes a nitric acid bath to dissolve any pyrite that may be left by the other acids. The other major difference is that the coal was not pyrolyzed before the demineralization treatment in Method II to avoid encapsulation of ash particles. An ultimate analysis of Demineralization Method II coal char is in Table 2.1.

The second coal demineralization method began with coal that has not been charred. It included the same concentrated hydrofluoric and hydrochloric acid baths as in the first method. The third bath of demineralization method II was a 1000 ml 18% nitric acid bath at 60°C, lasting for 1 hour while being stirred every 5 minutes. The resulting filter cake was washed with 10 L of distilled water, stirred overnight with 2 L of distilled water, washed again and pyrolyzed.

2.4. CATALYST IMPREGNATION

Potassium carbonate catalyzes the hydrogasification of coal chars particularly well. A 10 wt% catalyst loading was used on all catalyzed chars to achieve a K/C ratio of 0.02. This was done by combining 0.5-10 grams of sample with the appropriate amount of 0.1 M K_2CO_3 solution in a drying oven at 90°C. The samples were stirred every 45 minutes and removed when they appeared dry and no longer lost weight due to water evaporation.

2.5. HYDROGASIFICATION

2.5.1. GASIFICATION REACTOR SPECIFICATIONS

The hydrogasification reactor used for these experiments is an externally heated differential fixed bed reactor. The pressure vessel is made of Haynes-25 Cobalt alloy with a quartz liner inside. Samples were collected with a system of solenoid valves and a silica gel trapping medium, and analyzed with a gas chromatograph and chart recorder. The reactor, sample collection, and analysis systems are described in detail by Zoheidi.[93] Hydrogasification rate calculations are given in Appendix A.1.

2.5.1.1. GAS CHROMATOGRAPH

One of two modifications on the existing hydrogasification equipment during the course of this experimentation was the replacement of the F&M Model 810 Research Chromatograph with a Varian Analytical Instruments Model 3300 Gas Chromatograph. This chromatograph uses a thermal conductivity detector with a reference cell, and a Supelco 80/100 Carbosieve S-II stainless steel column, 5′x1/8", in parallel with a blank column. It also has an auto zero function which automatically establishes a baseline for the chart recorder. This makes interpretation of the raw data charts much easier. The column oven heating cycle used for all sample analyses consisted of an initial soak at 50Oc for 2 minutes, an increase from 50°C to 175°C at 20°C/min, and a final soak at 175°C for 2 minutes for a total time of 10.25 minutes.

2.5.1.2. SAMPLE MOUNT

The other modification to the existing equipment was a newly designed sample holder. The sample holder used in past studies was a ceramic hemispherical trough, 2.6 cm long, with a bed depth of 3 mm. It required a 325 mesh 316 stainless steel screen to be placed over the sample to help prevent blowout by high gas velocities. Disadvantages of this design included possible mass transfer limitations, small sample size, potential sample blowout, and metal in contact with the sample.

These problems were minimized or eliminated by using a cylindrical quartz chamber capped at both ends by 40-60 micron porous quartz frits. A diagram of the new sample holder is given in Figure 2. No metal parts come in contact with the chars. The reactant and purging gases are able to flow through the sample bed instead of over it, and cannot blow char out of the holder. A quartz wool

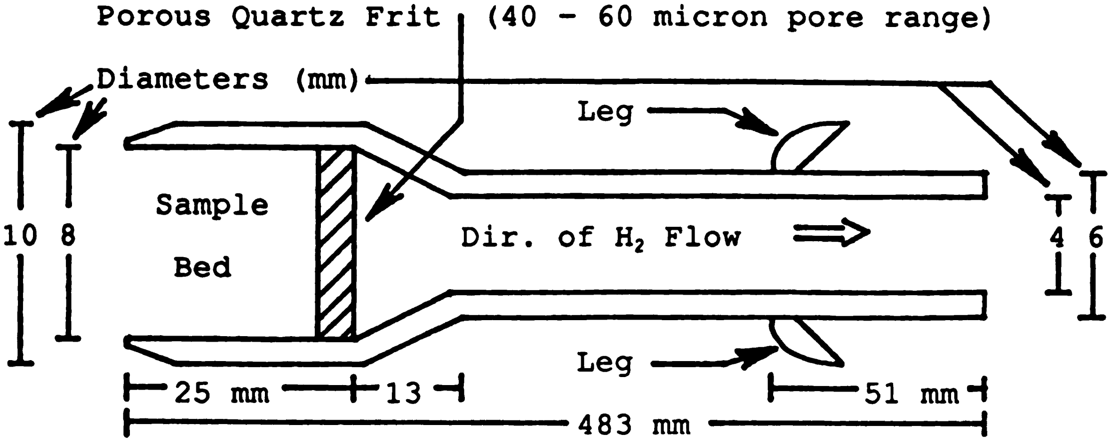

COMPONENT #1

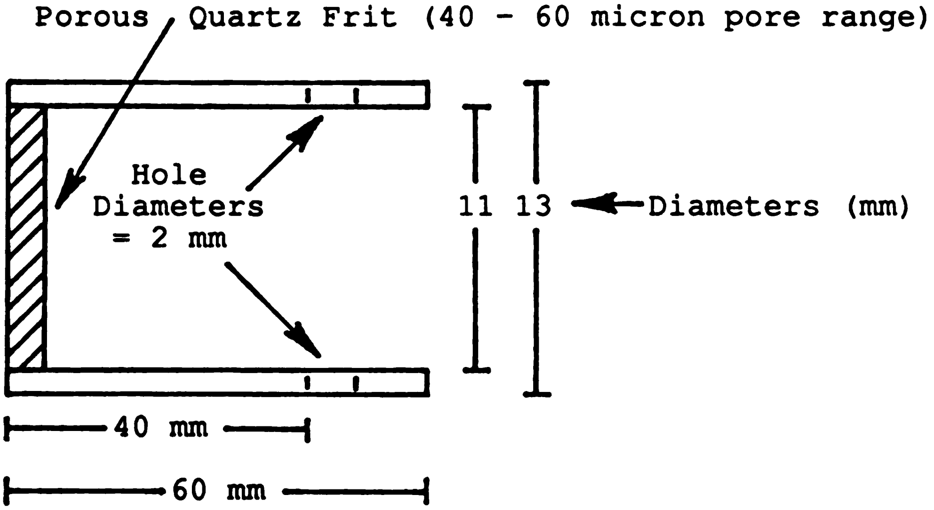

COMPONENT #2 - Fits over the wide end of Component #1.

Figure 2: Newly Designed Sample Holder

Material of Construction - Quartz

(figure not drawn to scale)

gasket seals the ring of contact between the two quartz components to prevent sample from being entrained. The components are held together by springs to ensure a tight seal.

The sample chamber volume is over four times greater than that of the ceramic sample mount, is variable, and does not require metal parts to come in contact with the chars. Insertion of small quartz frits and tubes in the chamber allows sample mass to vary greatly without causing empty spaces in the chamber. The only disadvantage is that chars must be sieved to greater than 200 mesh size so that smaller sample particles do not clog or pass through the frits. This eliminates roughly half of the prepared char mass that can be used for hydrogasification.

2.5.2. HYDROGASIFICATION KINETIC EXPERIMENTS

2.5.2.1. CONDITIONS

All gasification experiments were conducted at 725°C and 500 psig under pure hydrogen at a flowrate of 300 cc(STP)/min unless otherwise indicated. A temperature of 725°C was used because temperatures lower than this result in reaction rates that are too slow, while temperatures higher than this can result in mass transfer limitations for this reaction system. A pressure of 500 psig was used because pressures below this result in slow reaction rates, while pressures above this approach the safety limitations of the reaction vessel, and methane may not remain the greatly favored product.[7] A flowrate of 300 cc(STP)/min ensures that fractional conversion of hydrogen will be low enough to observe intrinsic kinetics, and the influence of methane on the reaction can be minimized. Calculations of the fractional conversion of hydrogen at these conditions have been done by Zoheidi.[93]

2.5.2.2. PROCEDURE

Samples were weighed and loaded into the reactor which was then purged with helium before gasification. After 15-20 minutes the reactor was evacuated to 30"Hg vacuum and the furnace was turned on to a setpoint of 600°C. Another helium purge was started after the evacuation. During this time the sample traps and gas chromatograph columns were cleaned, then a calibration run was made. The calibration gas used for all runs was 4.8% CH_4, 4.9% CO, 4.9% CO_2, and balance He. The furnace typically reached a temperature of about 525°C by the end of the calibration, at which time it was set to 725°C. The helium purge was stopped, the reactor was filled with hydrogen when it reached a temperature of 600°C, and the first sample was taken at 650°C. Most effluent gas sample collection times were one minute with 15-20 minutes between collections, but times varied depending upon the rate of methane formation during a particular reaction. Other procedures varied slightly depending upon gasification temperature, pressure, and intermittent treatments. At the end of a designated time period the furnace and hydrogen were both shut off simultaneously, and the reactor was purged with helium for 15-20 minutes and allowed to cool to room temperature overnight. Most gasifications proceeded for 2.25 hours, but some proceeded longer for higher conversions.

2.5.3. OUTGASSING

Outgassing was used as a pretreatment or an intermittent treatment to remove oxygen functional groups from Saran char and coal char surfaces. This was done to study the reactivity of the bulk char and the effects of surface annealing. Ten to fifteen grams of sample were set inside the hydrogasification reactor, which was purged with helium. The reactor was then placed under 30"Hg vacuum and heated to 1000°C for 16 hours, during which vacuum was continuously being applied. It was then followed by another helium purge. Outgassing was used as a pretreatment or an intermittent treatment for some hydrogasifications.

2.6. SURFACE ANALYSIS

2.6.1. TOTAL SURFACE AREA

Carbon dioxide physisorption was used to determine the total surface area of sample chars. Samples were first outgassed to remove water and other contaminants which occupy pore volume. Next, they were weighed under vacuum in an electronic microbalance. The samples were then exposed to carbon dioxide at predetermined pressure increments and weighed at each increment. Data was analyzed with the Dubinin-Radushkevitch method to calculate total surface area. Greater detail on this and other surface analysis techniques are given by Toomajian.[113]

2.6.2. ACTIVE SURFACE AREA

Oxygen chemisorption was used as a method to determine the active surface area of various samples, because desorption of oxygen from char surfaces prior to and during hydrogasification is believed to create active sites where gasification takes place. Samples were first outgassed in an inert atmosphere at 725°C to clean them of surface contaminants. They were then put through a temperature programmed desorption to determine how clean the char surfaces were and at what temperature various oxygen groups desorb. Pulses of a known amount of oxygen were then passed over the sample at 295°C and analyzed to determine the amount that had chemisorbed. This temperature was chosen because it is high enough to facilitate chemisorption, but not high enough to cause excessive combustion of the char. Oxygen chemisorption has also been used as form of oxidative sample treatment for some hydrogasifications in this study.[113]

2.6.3. SURFACE OXYGEN CONCENTRATION

X-ray photoelectron spectroscopy was used to determine the oxygen to carbon ratio on char surfaces. A monochromated magnesium x-ray source was used in early tests, but better analysis was made possible with a monochromated aluminum x-ray source which was used in later tests. Samples were outgassed in a vacuum pretreatment reactor prior to analysis to remove loosely physisorbed surface contaminants. A survey scan was the first analysis performed on a char sample, which determined overall sample elemental composition by analysis of data over a wide range of energy levels. The second analysis performed on a char sample was a multiplex scan, which determined bonding states of specific elements by focusing on a narrow band of energy levels.[113]

2.6.4. SURFACE pH

This test, ASTM method D3838-80, determined the acidity or basicity of the functional groups on char surfaces. It consisted of immersion of the char in a 0.1 M potassium chloride solution for two hours under reflux. After the solution was cooled to 23°C, surface pH was measured and compared to the pH of a 0.1 M KCl standard solution that had undergone the same treatment. A positive change in pH (pH of sample solution minus pH of standard solution) indicated basic functional surface groups, while a negative change in pH indicated acidic groups. This test only provided information on the general nature of surface functional groups, it did not provide information on individual types.[113,115]

CHAPTER 3

RESULTS

Results of gasification experiments are presented in this chapter. After establishing that kinetic rate measurements are dominated by reaction and not mass transfer, the effects of outgassing, preoxidation, and intermittent oxidation are reported. Following these, results at lower temperature, rates following hydrogen pretreatment, and effects of catalyst addition are given.

3.1. EFFECT OF TEMPERATURE

Figure 3 contains rate data on the hydrogasification of coal char at 7% conversion. Temperature varies from 800°C at the far left to 700°C by increments of 25°C. A conversion of 7% was chosen because the reaction does not reach steady state until 6% conversion at 800°C, and conversions higher than 7% do not give as large a separation between rate data points because of the rapid

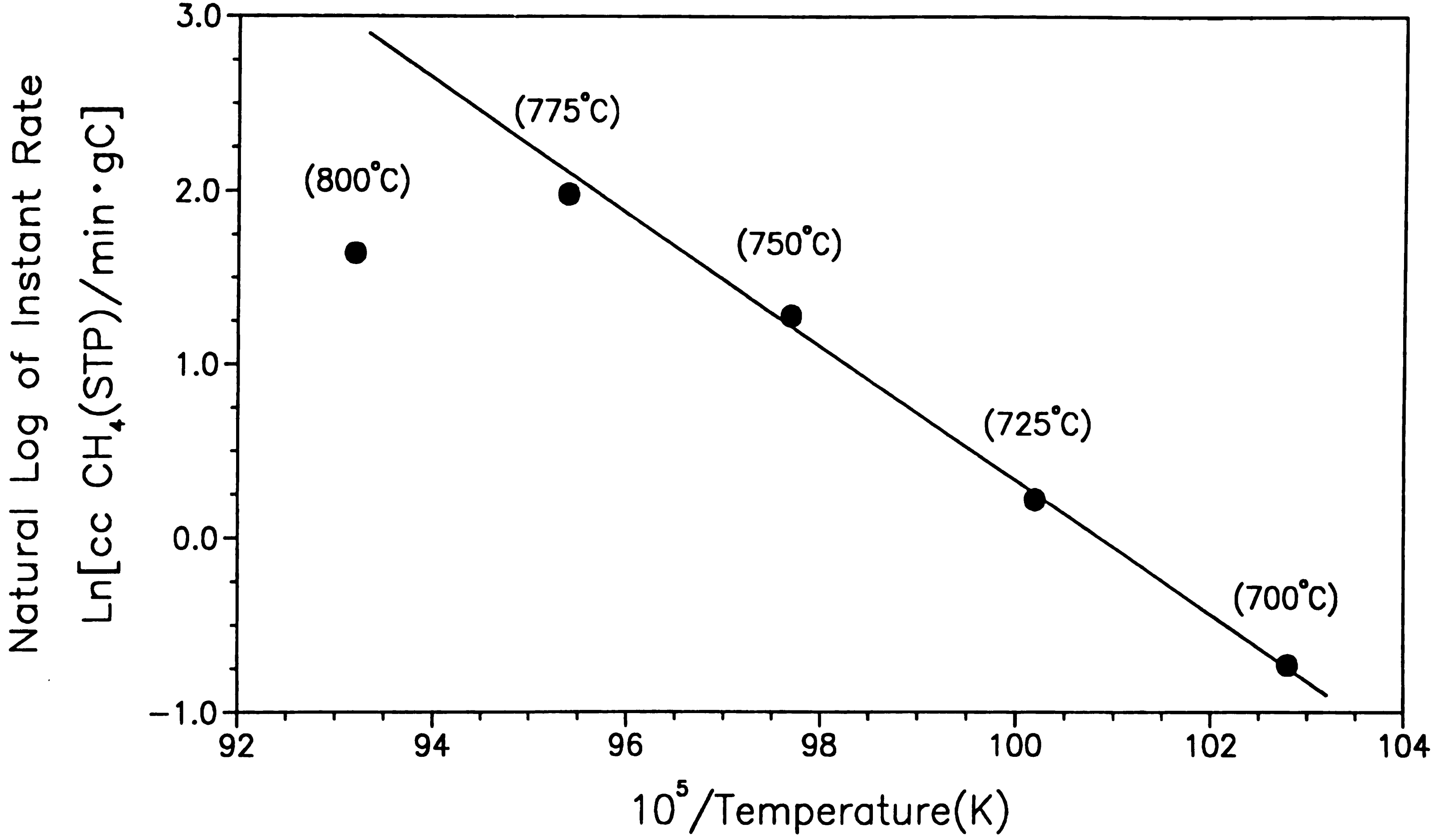

Figure 3: Arrhenius Plot of Coal Char at 7% Conversion (E_A=76kcal/gmol)

deactivation of the reaction. The maximum temperature at which diffusion limitations do not affect the reaction rate is 775°C. The temperature of all hydrogasifications performed in this investigation was at or below 725°C to remain well within kinetic rate limitations. The activation energy based on a slope which excludes the data point on the far left is 76 kcal/mol carbon, which is close to values reported for intrinsic gasification rates by other investigators.[17,18]

3.2. BASE CASE CHAR REACTIVITY

Hydrogasification rate is shown as a function of carbon conversion in Figure 4 for Saran char and three coal chars. The Saran char and coal char were just pyrolyzed, while the other coal chars were demineralized. The Saran char has been gasified for 8 hours. The coal char and Demin. II coal char have both been gasified for 9 hours, while the Demin. I coal char has been gasified 2.25 hours. Rate is reported as cubic centimeters of methane (STP) per minute per gram carbon present. All chars react at similar rates and have similar rate decay patterns. The Demin. II char rate curve is shifted outward slightly from the others. This may be due to residual effects of HNO_3 oxidation [48] that survived pyrolysis, or a greater

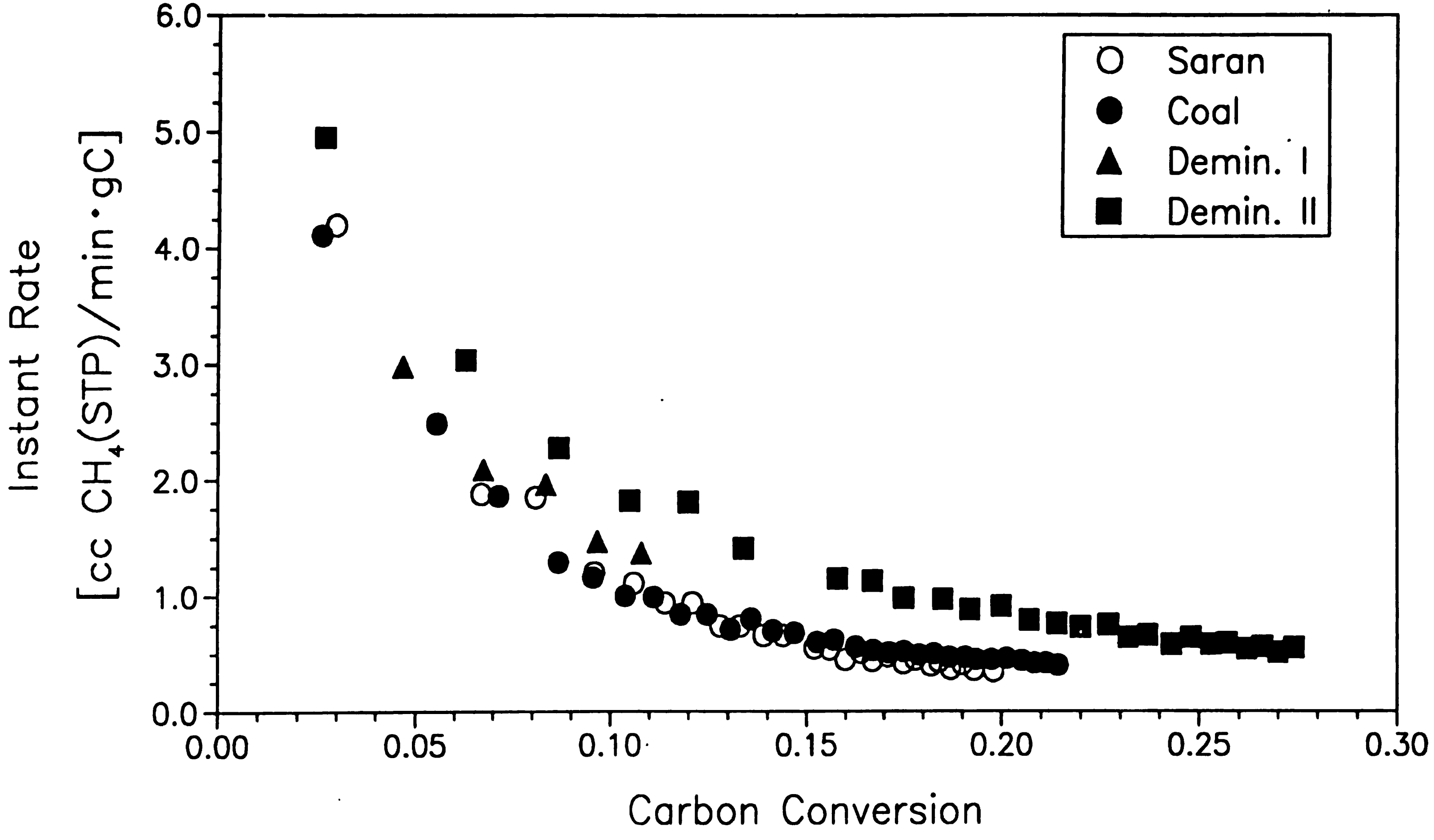

Figure 4: Hydrogasification of Various Chars at 725°C and 500 psi H_2

amount of active surface area exposed by the removal of ash particles.

3.3. OUTGASSING

3.3.1. SARAN CHAR

The effect of outgassing on the hydrogasification rate of Saran char is shown in Figure 5. The 8 hour base case run was not pretreated, but has been included as a basis for comparison. The outgassed Saran char was gasified for 4 hours, at a rate that was about an order of magnitude less than the base case Saran Char. The intermittent treatment consisted of a flash desorption to 1000°C for 15 minutes in helium under a 30" Hg vacuum after 2.25 hours of gasification. This treatment decreased the reaction rate of the Saran char to about 1/5 the rate of the base case.

3.3.2. COAL CHAR

The effect of outgassing on the hydrogasification rate of coal char is shown in Figure 6, and the results are similar to those of Saran char. The outgassed coal char reacted at a rate which was an order of magnitude

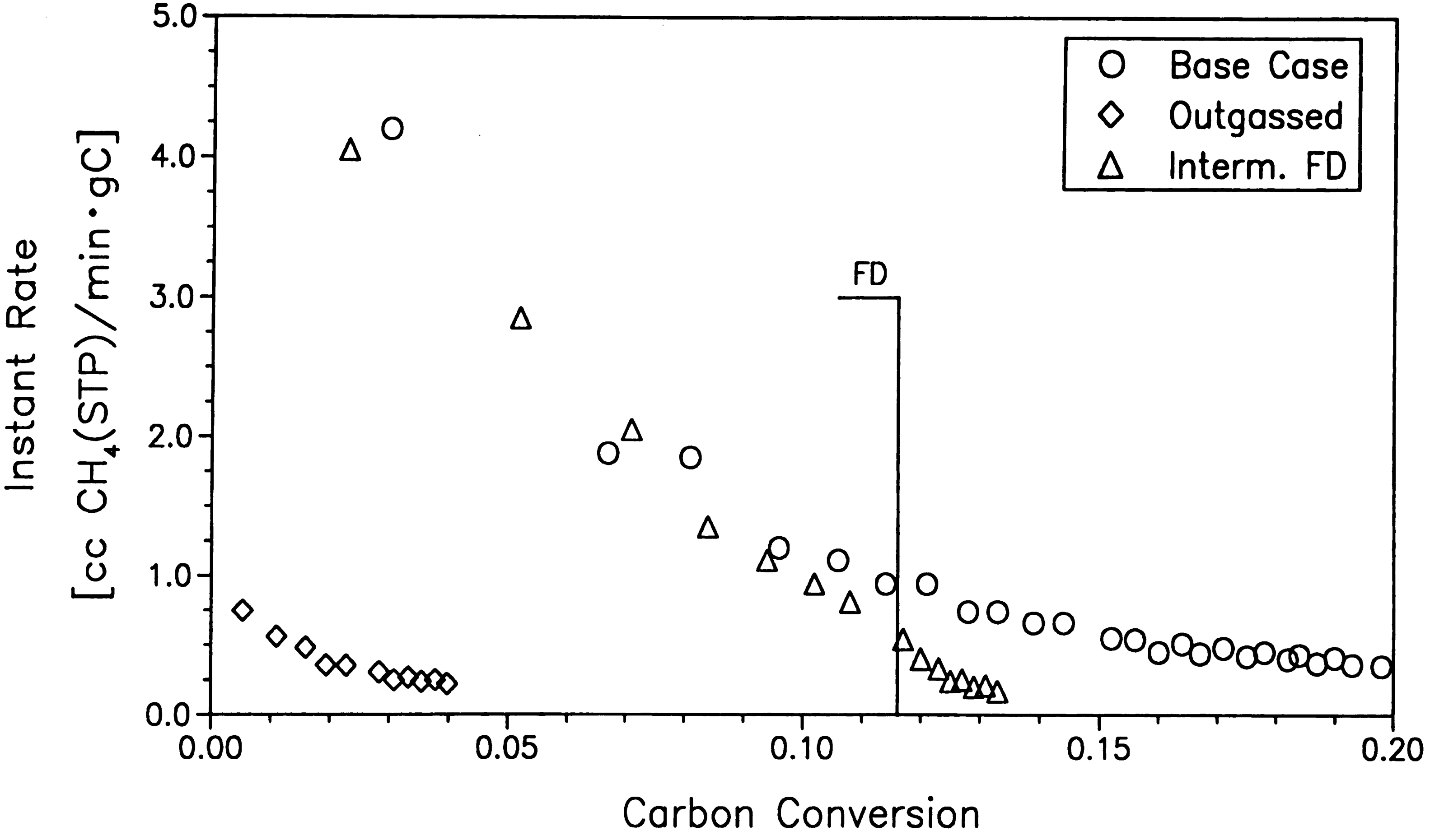

Figure 5: Effect of Outgassing on Hydrogasification of Saran Char

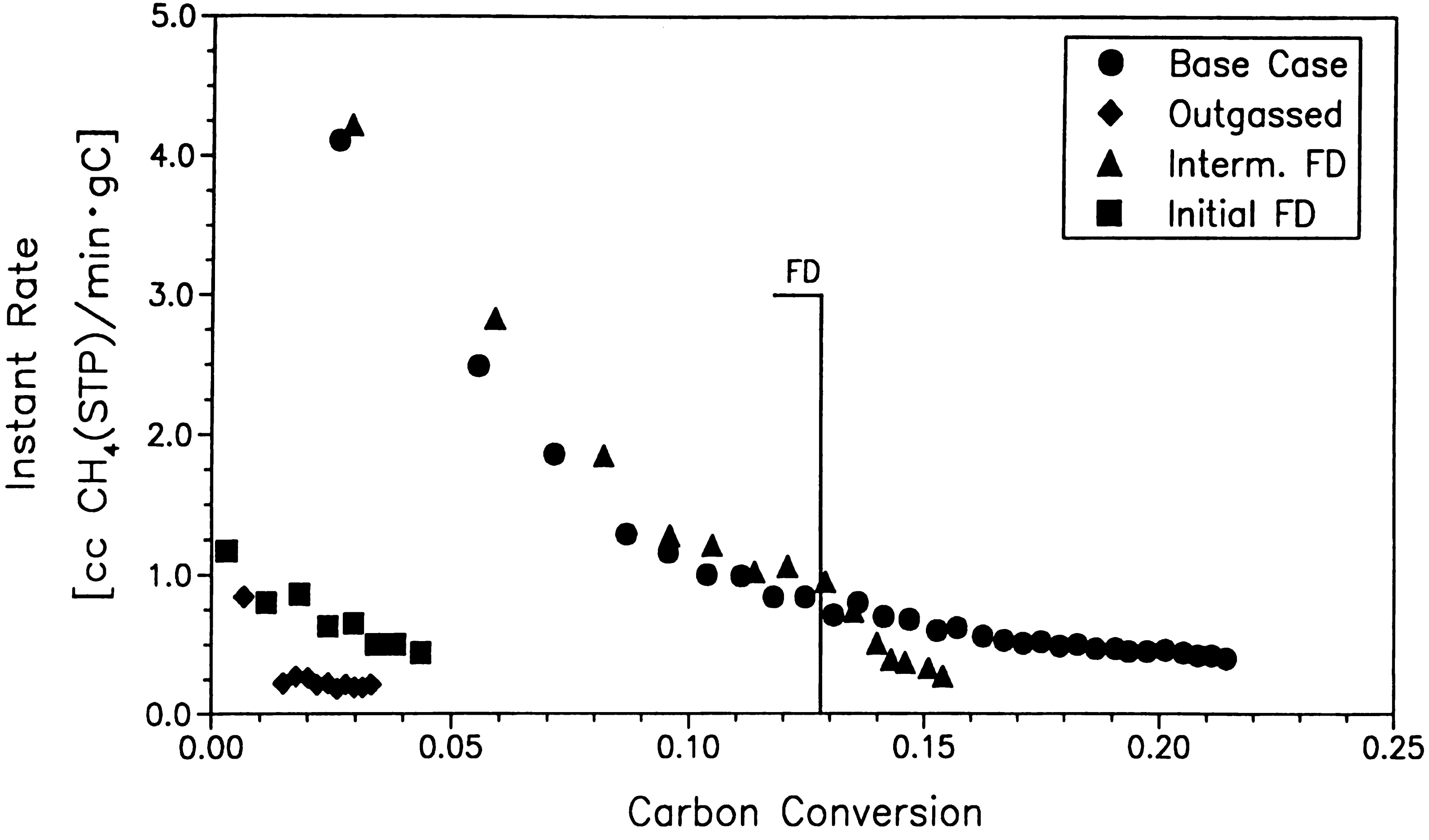

Figure 6: Effect of Outgassing on Hydrogasification of Coal Char

less than the base case, and the intermittent flash desorption decreases the reaction rate to about half that of the base case.

3.4. OXIDATIVE TREATMENTS

3.4.1. OXIDATIVE PRETREATMENTS

Figures 7 and 8 show the results of oxidative pretreatment of various chars by partial combustion in air. Figure 7 shows percent weight loss of chars as a function of the length of time they have been exposed to flowing air at 375°C. The percent weight loss is a weighted average of all five trays which contain char during oxidation. The relationship between time of air flow and percent weight loss appears to be fairly linear over the range of data present. Figure 8 shows the same six partial oxidation runs, but the percent weight loss for each run is broken down into individual trays. The trays were numbered in order from one to five and arranged so that the direction of air flow was always from tray #1 to tray #5. Most plots are parabolic in shape, with maxima at tray #3. This results from the parabolic temperature profile within the heated zone of the furnace.

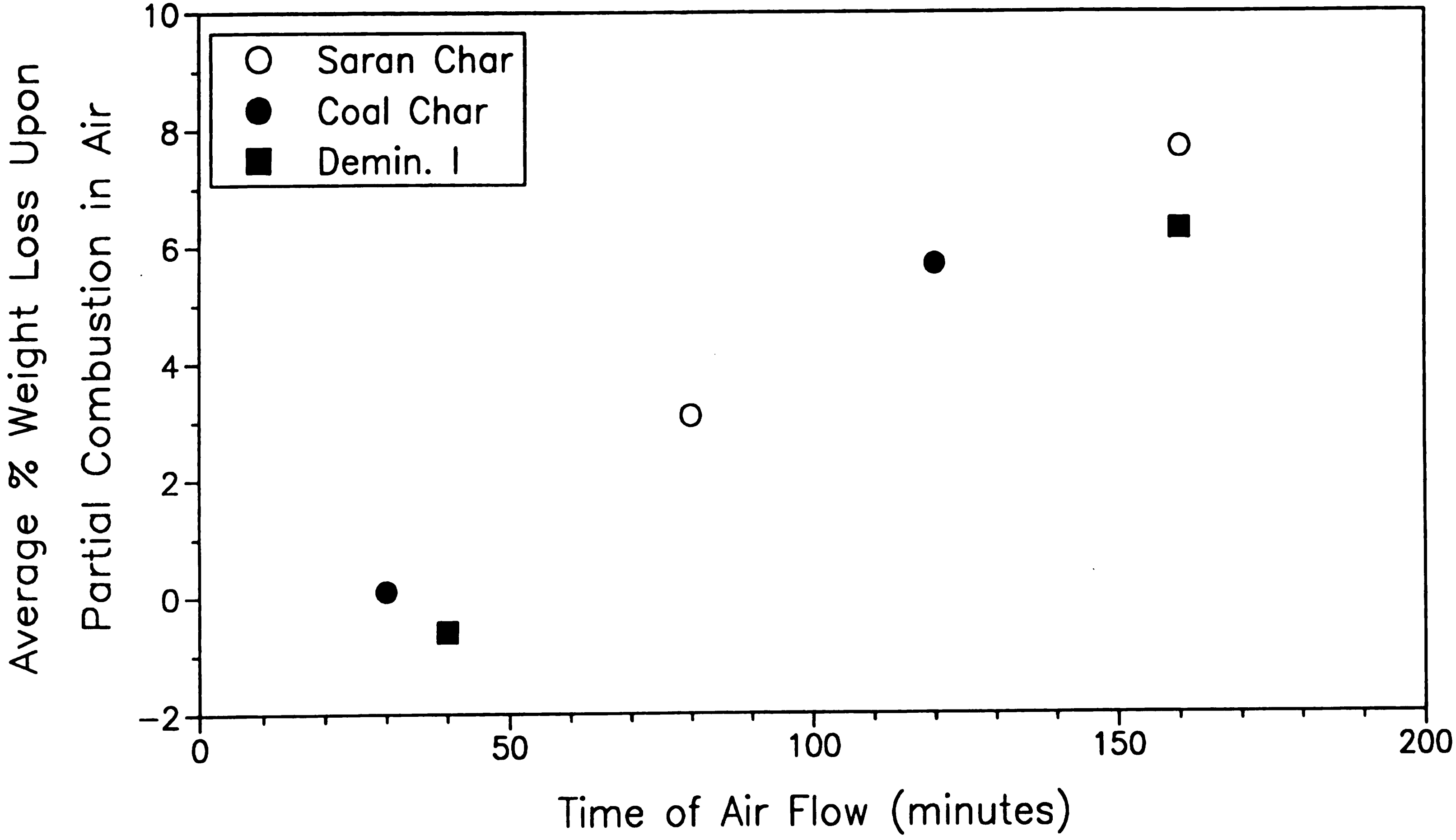

Figure 7: Weight % Burnoff of Various Chars in Air at 375°C

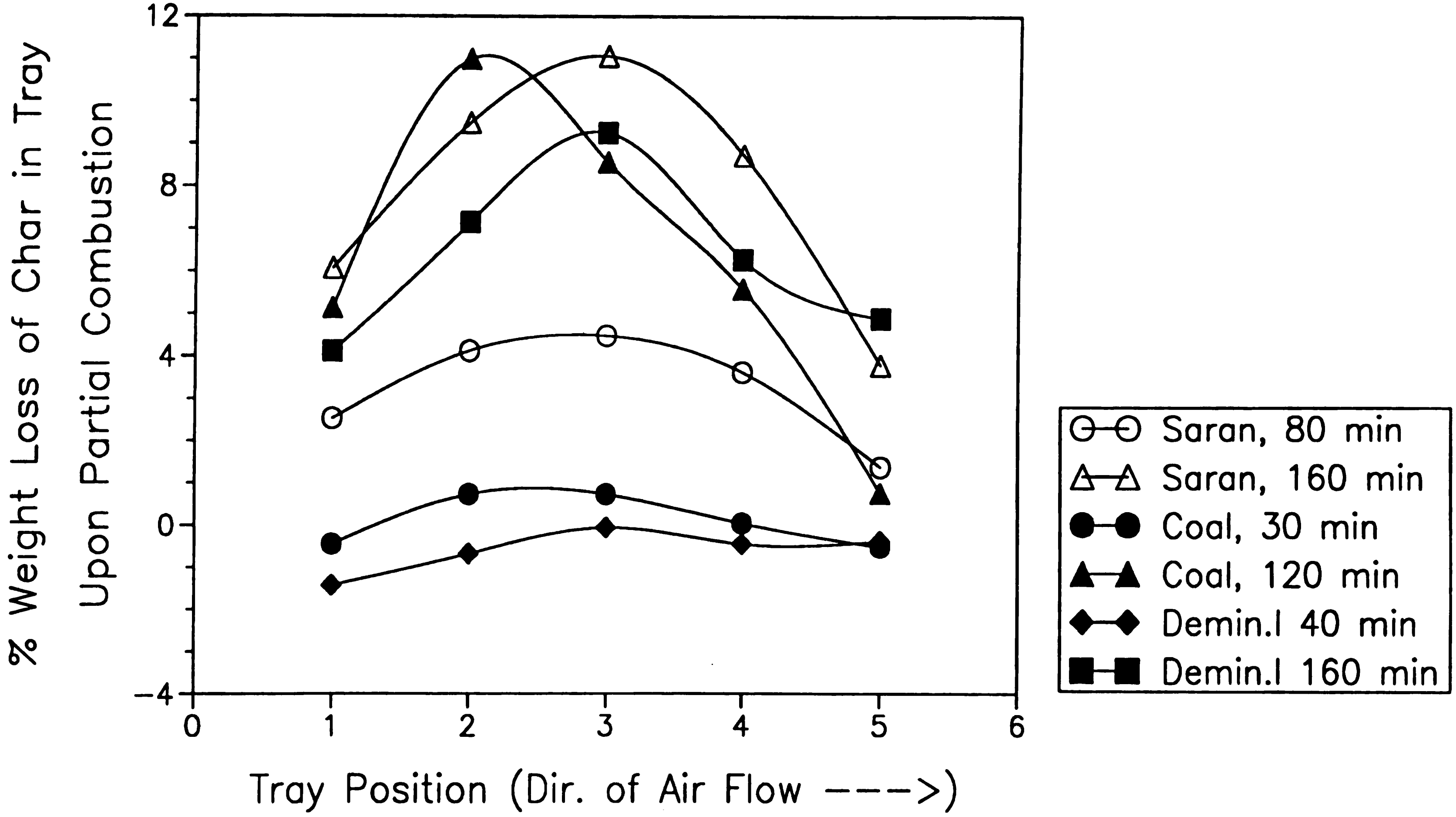

Figure 8: Weight % Burnoff of Individual Trays of Various Chars in Air at 375°C

3.4.1.1. SARAN CHAR

Figure 9 gives the effects of oxidative pretreatments on the hydrogasification rates of Saran char. Two samples were partially oxidized in air at 375°C. One lost 3.1 wt% upon partial combustion, while the other lost 7.7 wt% because it was burned longer. The rate curves may be shifted slightly, but there was basically no rate enhancement in gasification resulting from these pre-oxidations. The other sample was first outgassed, then oxidized in air at 375°C before hydrogasification. The outgassed Saran char sample that was not preoxidized is included as a basis for comparison. The rate of the outgassed, then preoxidized sample was several times lower than the base case, but was 2-3 times higher than the outgassed sample.

3.4.1.2. COAL CHAR

The effects of oxidative pretreatment upon the hydrogasification rates of coal char can be seen in Figures 10 and 11. The first oxidation method used was partial combustion in air at 375°C for two different time periods. Weight losses were 0.1 wt% and 5.7 wt% during oxidation. The second method was partial combustion in air at 725°C to 3.7 wt% burnoff. The third was an oxygen

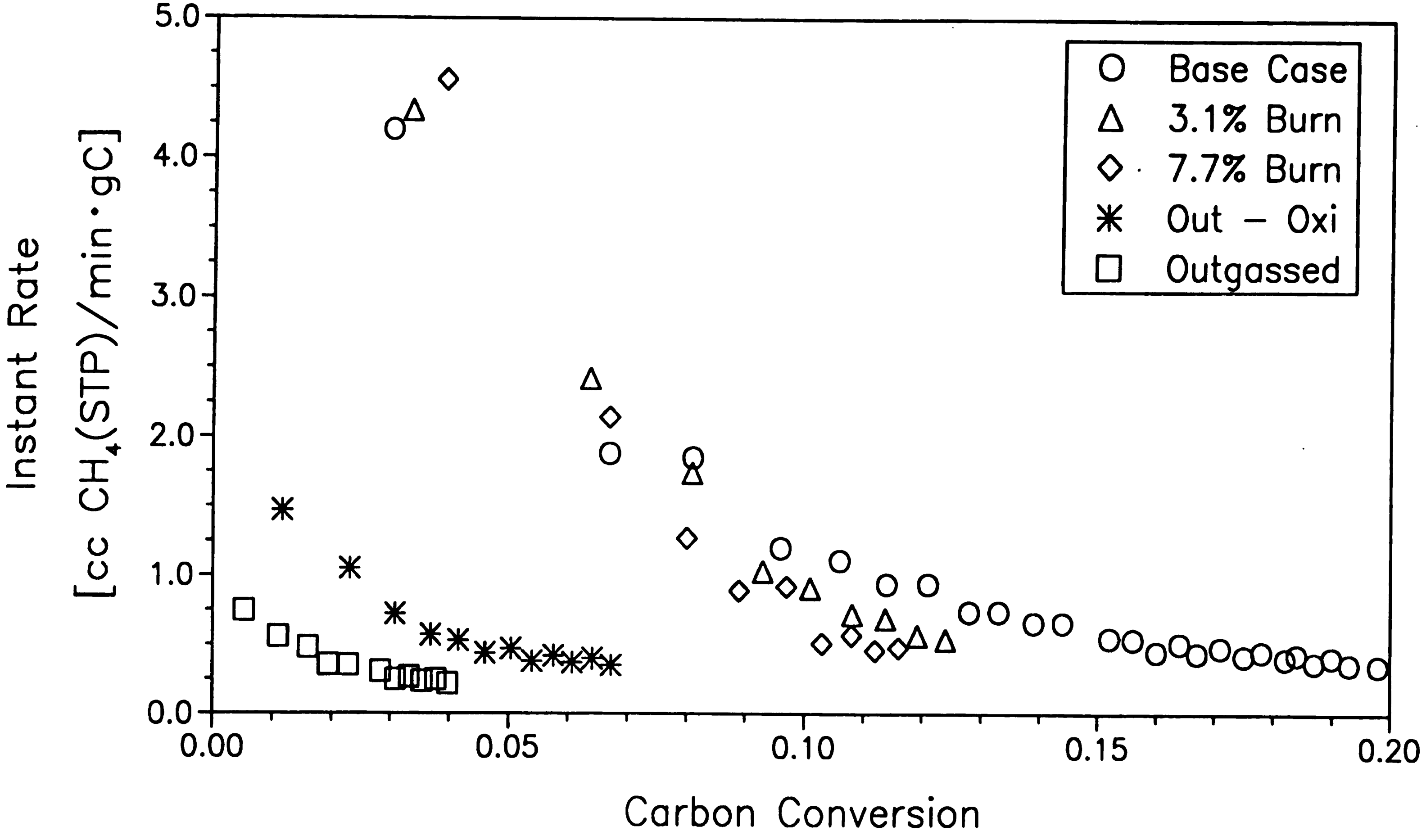

Figure 9: Effect of Oxidative Pretreatment at 375°C on Hydrogasification of Saran Char

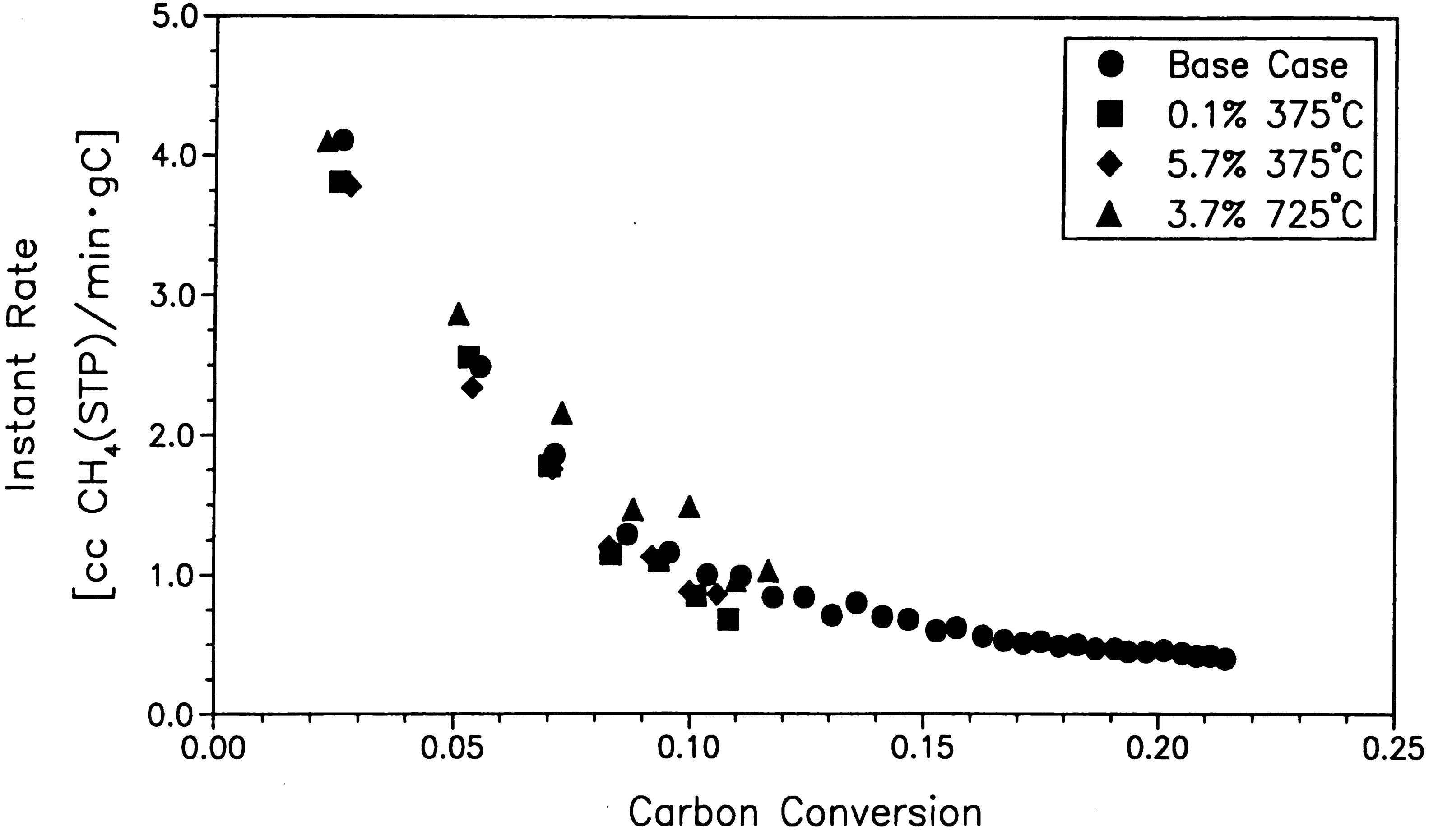

Figure 10: Effect of Oxidative Pretreatment at 375°C and 725° on Hydrogasification of Coal Char

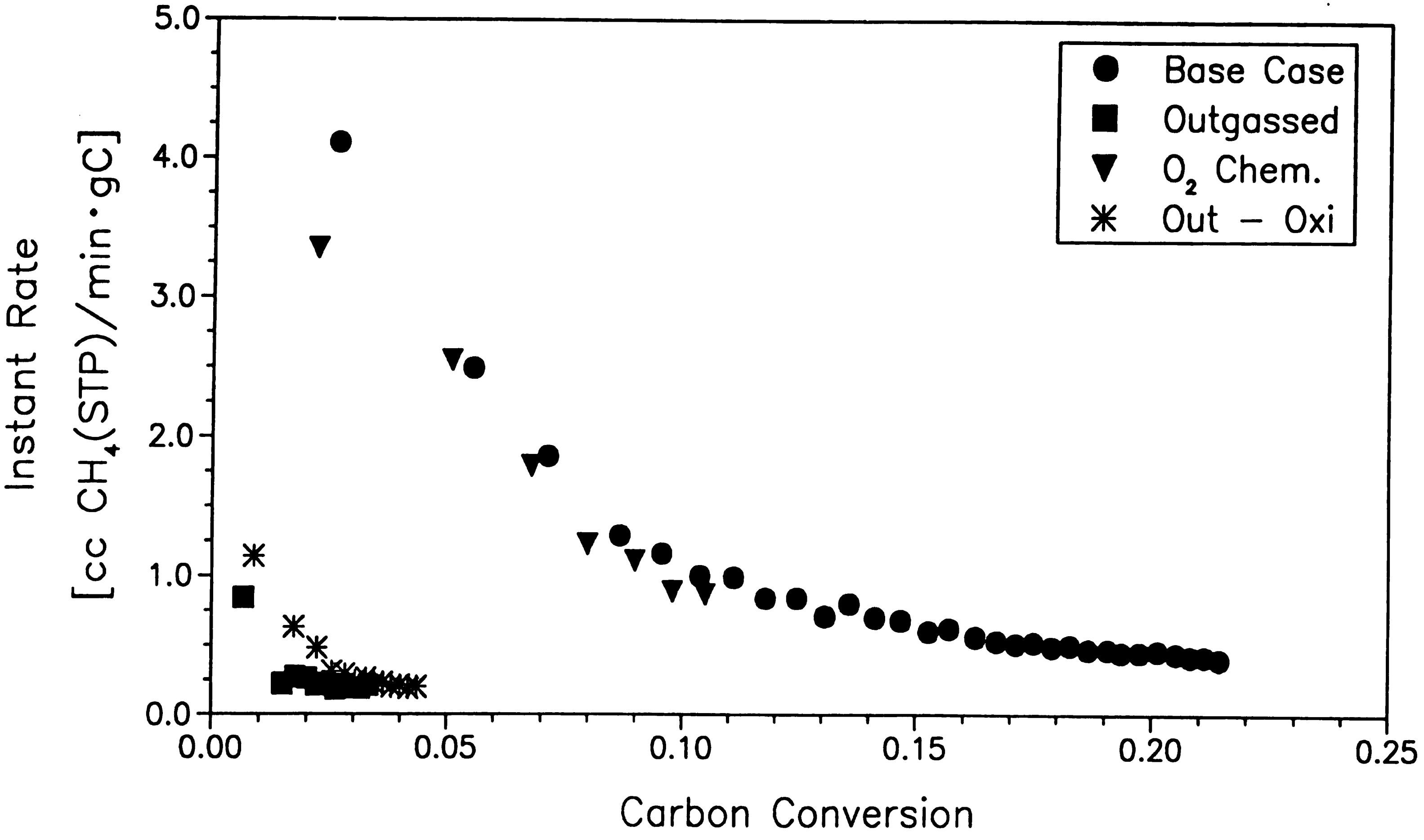

Figure 11: Effect of Oxidative Pretreatment at 375°C on Hydrogasification of Coal Char

chemisorption, while the fourth was an outgassing followed by a partial combustion in air at 375°C. As with Saran char, preoxidation of coal char did not result in any rate enhancement. The sample that had been outgassed and then preoxidized in air at 375°C did show some hydrogasification rate enhancement over the coal char that had just been outgassed, but the enhancement was not as great as that of the Saran char.

3.4.1.3. DEMINERALIZED COAL CHAR

The effect of oxidative pretreatment on the hydrogasification rate of coal char demineralized via Method I is shown in Figure 12, and via Method II in Figure 13. All pretreated samples were partially reacted in air at 375°C for varying lengths of time. Neither of the demineralized coal chars show enhanced rates due to oxidative pretreatment.

3.4.2. INTERMITTENT OXIDATIVE TREATMENTS

3.4.2.1. SARAN CHAR

Figure 14 shows the effect of intermittent oxidation at 375°C on the hydrogasification rate of Saran char. Gasification proceeded for 2.25 hours between successive

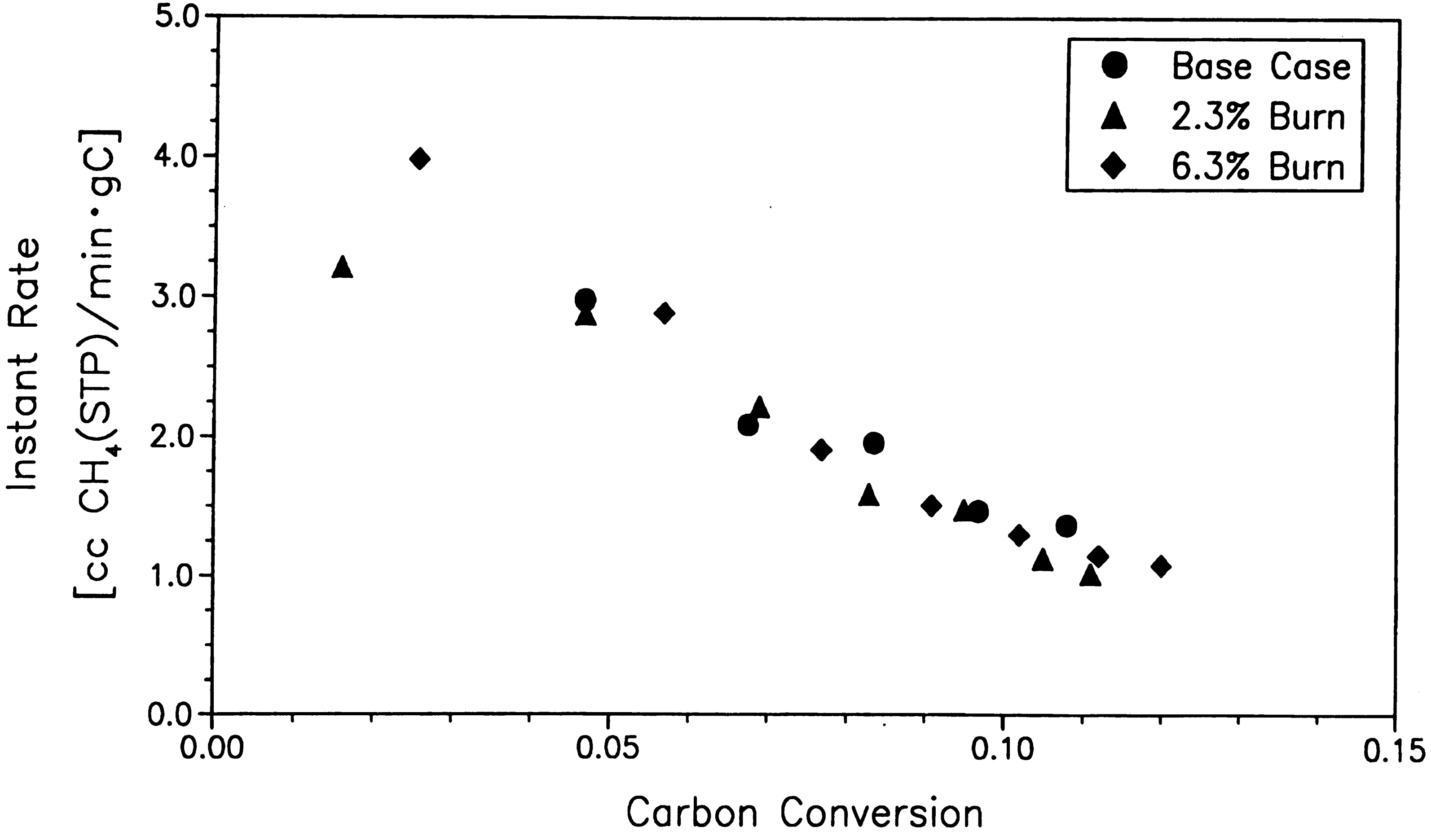

Figure 12: Effect of Oxidative Pretreatment at 375°C on Hydrogasification of Demineralized Coal Char (Method I)

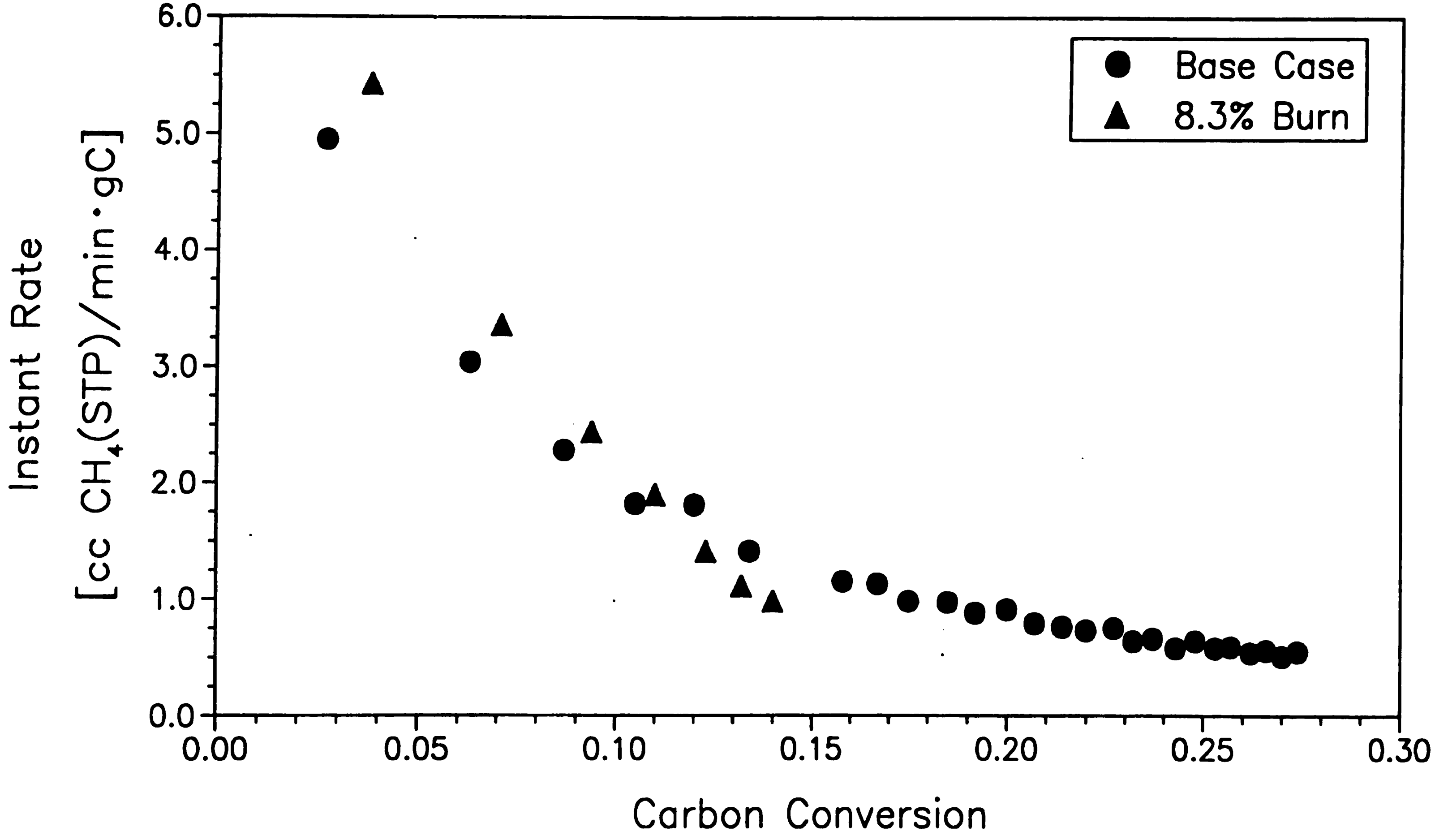

Figure 13: Effect of Oxidative Pretreatment at 375°C on Hydrogasification of Demineralized Coal Char (Method II)

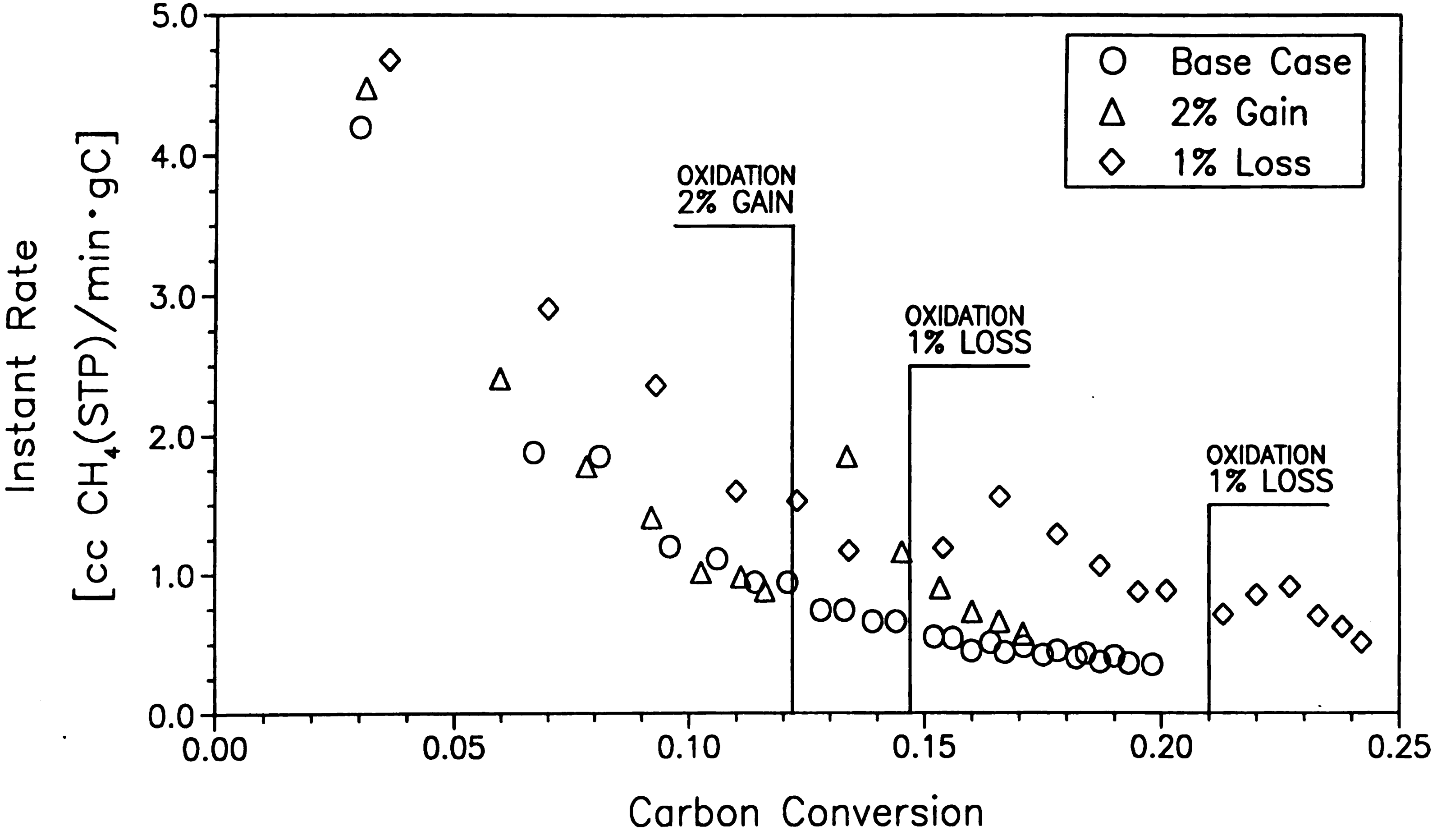

Figure 14: Effect of Intermittent Oxidation at 375°C on Hydrogasification of Saran Char

oxidations. The first intermittently treated sample gained 2 wt% upon oxidation, while the second sample was intermittently treated longer and lost 1 wt% during each oxidation. Figure 15 shows the effect of intermittent oxygen chemisorption on the hydrogasification rate of Saran char. After all intermittent oxidations, the rates increased 2-3 fold over the base case, but decayed back to the base rate after about 5% carbon conversion.

3.4.2.2. COAL CHAR

Intermittent oxidative treatments are shown for coal char in Figures 16 and 17. Gasification proceeded for 2.25 hours between successive oxidations. The samples in Figure 16 were oxidized two times at 375°C during each reaction. The first lost 7 wt% both times upon combustion in air, and the second lost 5 wt% during each oxidation. Figure 17 gives the hydrogasification rare curve for coal char that has been partially burned in air at 725°C. This sample lost 3 wt% during the oxidation. As with the Saran char, all rates increased 2-3 times over the base case following intermittent treatment and decayed back to the base rate after approximately 5% carbon conversion.

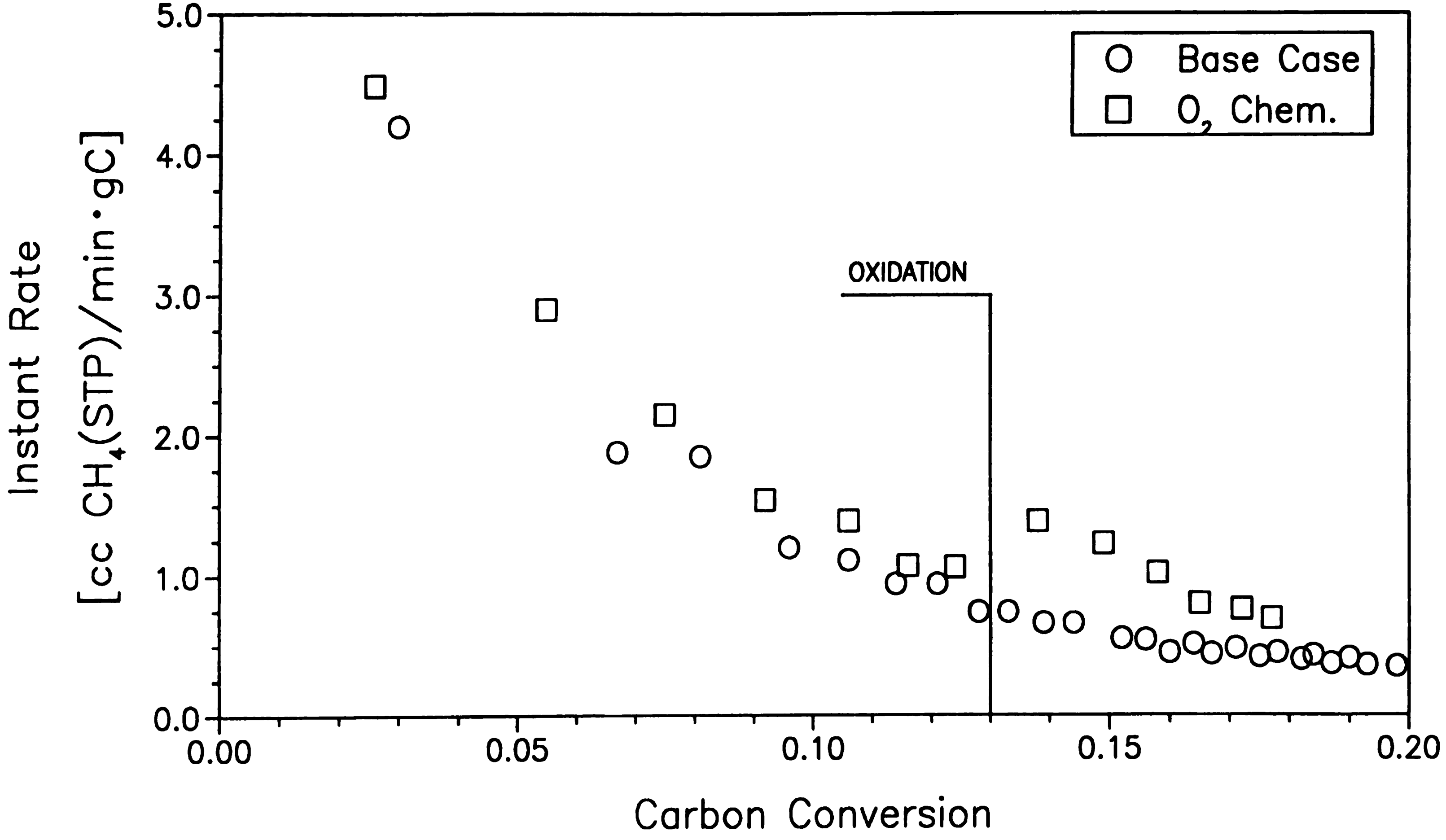

Figure 15: Effect of Intermittent Oxygen Chemisorption on Hydrogasification of Saran Char

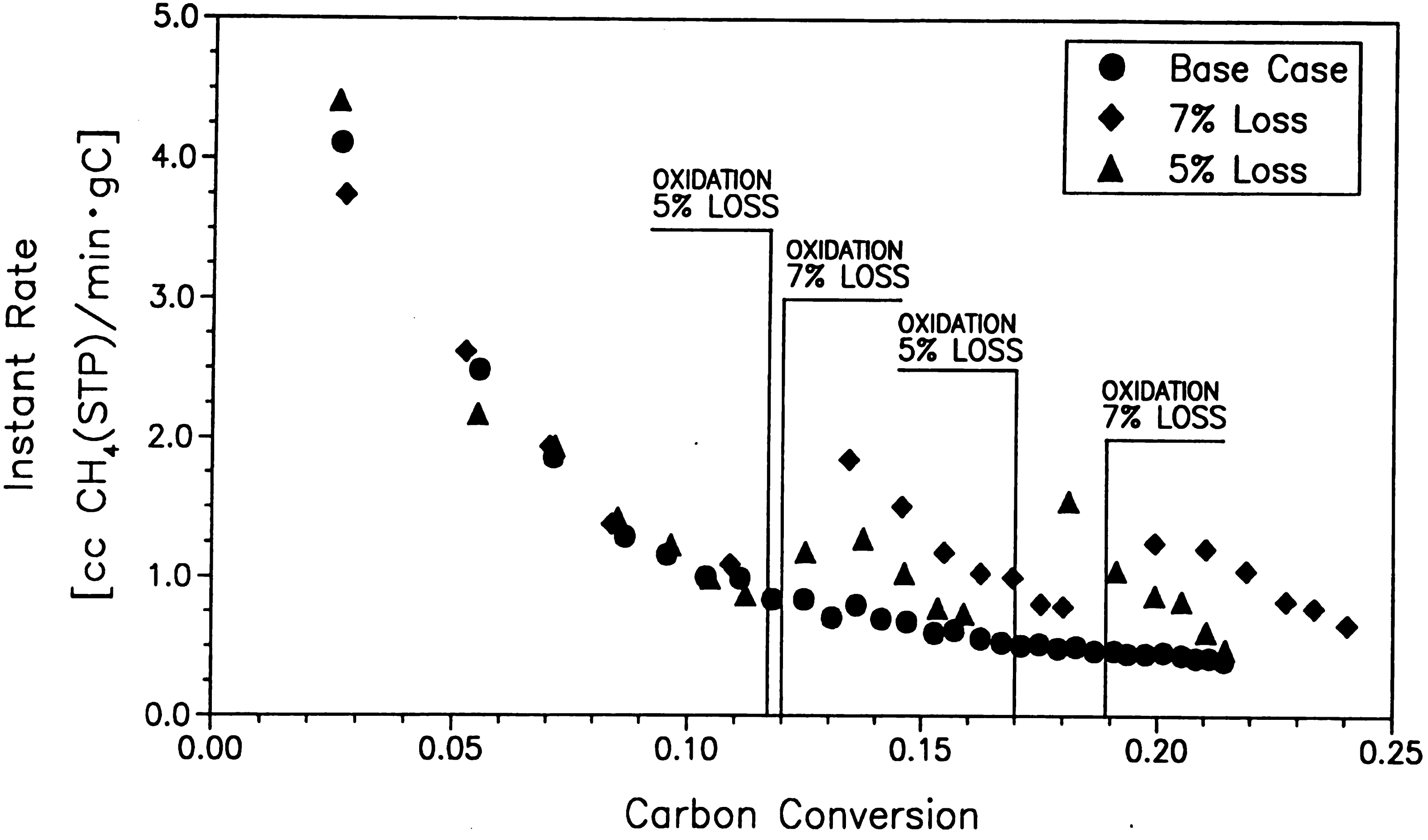

Figure 16: Effect of Intermittent Oxidation at 375°C on Hydrogasification of Coal Char

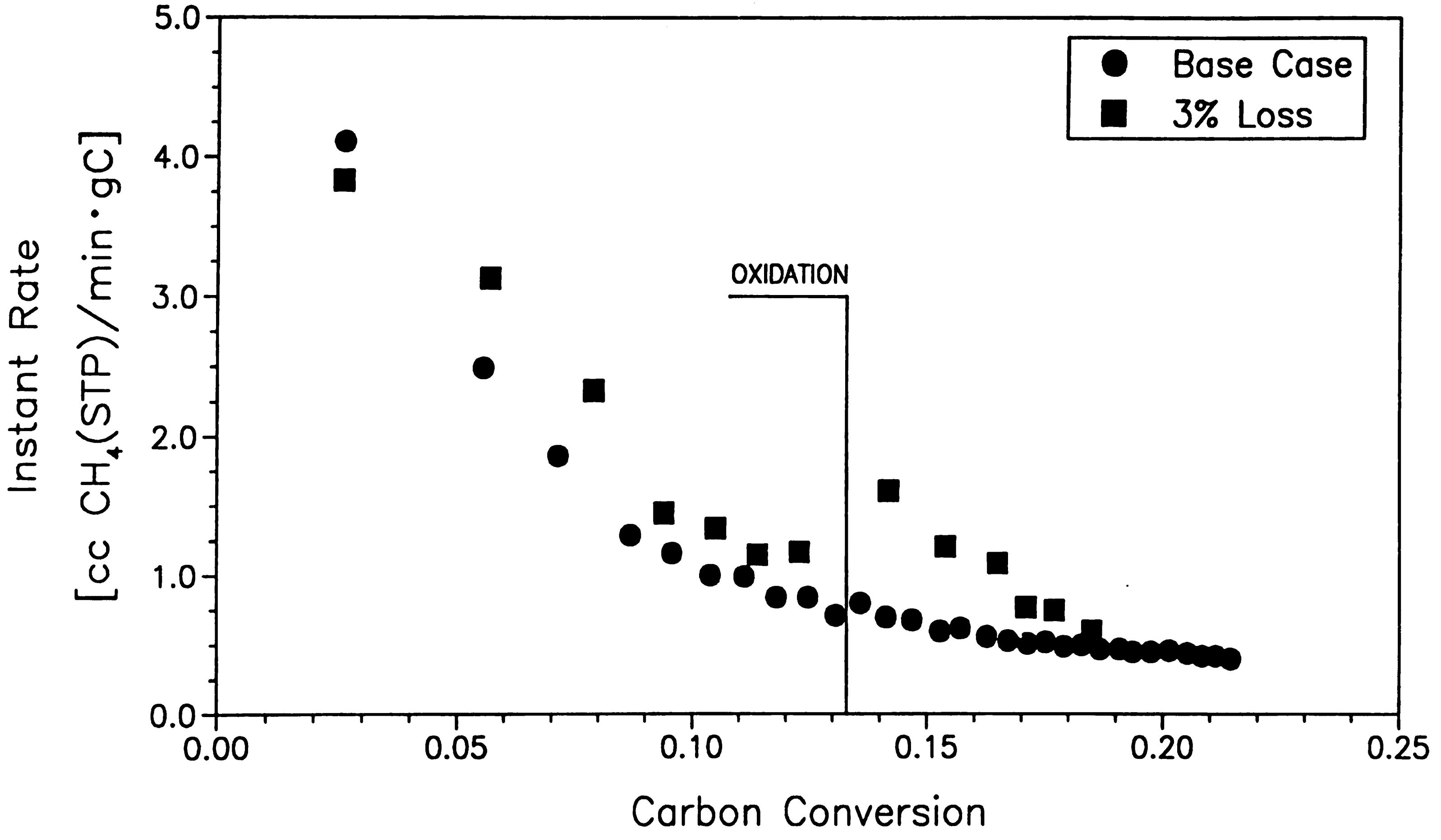

Figure 17: Effect of Intermittent Oxidation at 725°C on Hydrogasification of Coal Char

3.5. HYDROGEN ADDITION AT STEADY STATE REACTION TEMPERATURE

An advantage of using the newly designed sample mount during hydrogasification is having the option of adding hydrogen to the reactor as quickly as possible and not having some of the sample blow out of the holder before 500 psi is achieved. The standard procedure used in this study for gasifying samples was developed before the design of the new sample mount, making slow addition of hydrogen starting at 600°C the best method. Figure 18 shows the effect on hydrogasification rate of adding 500 psi hydrogen very quickly to the reactor when it has just reached 725°C. The initial recorded reactivity of coal char is almost twice as high as that of the base case, but the rest of the rate points fall closely to those of the base case.

3.6. REDUCED GASIFICATION TEMPERATURE

Figure 19 shows the effect of reducing hydrogasification temperature to 600°C on the reaction rate of Saran char, coal char, and pre-oxidized coal char. The pre-oxidized coal char has been burned in air at 375°C

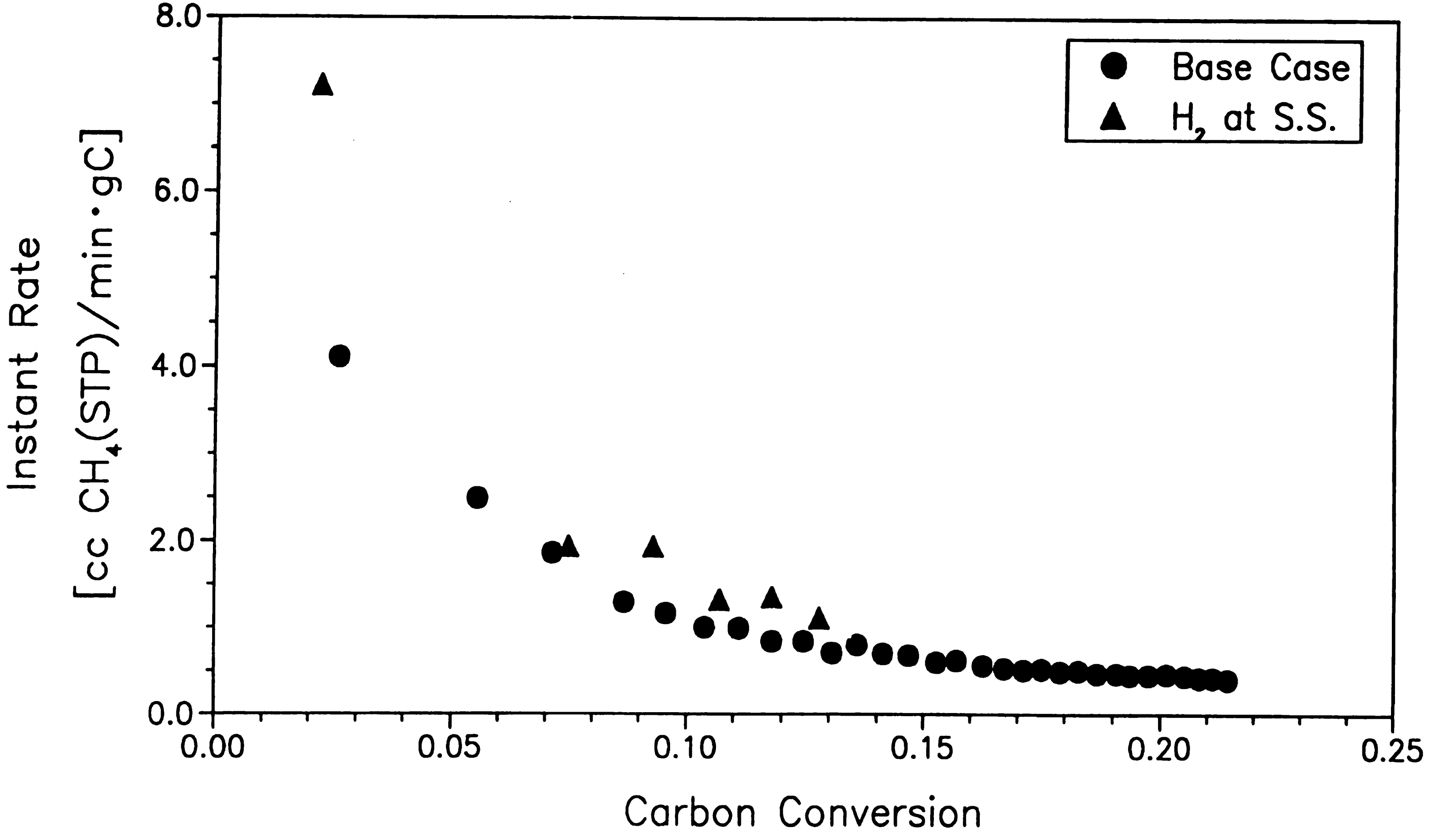

Figure 18: Effect of Addition of 500 psi H_2 at Steady State Reaction Temperature (725°C) on Coal Char

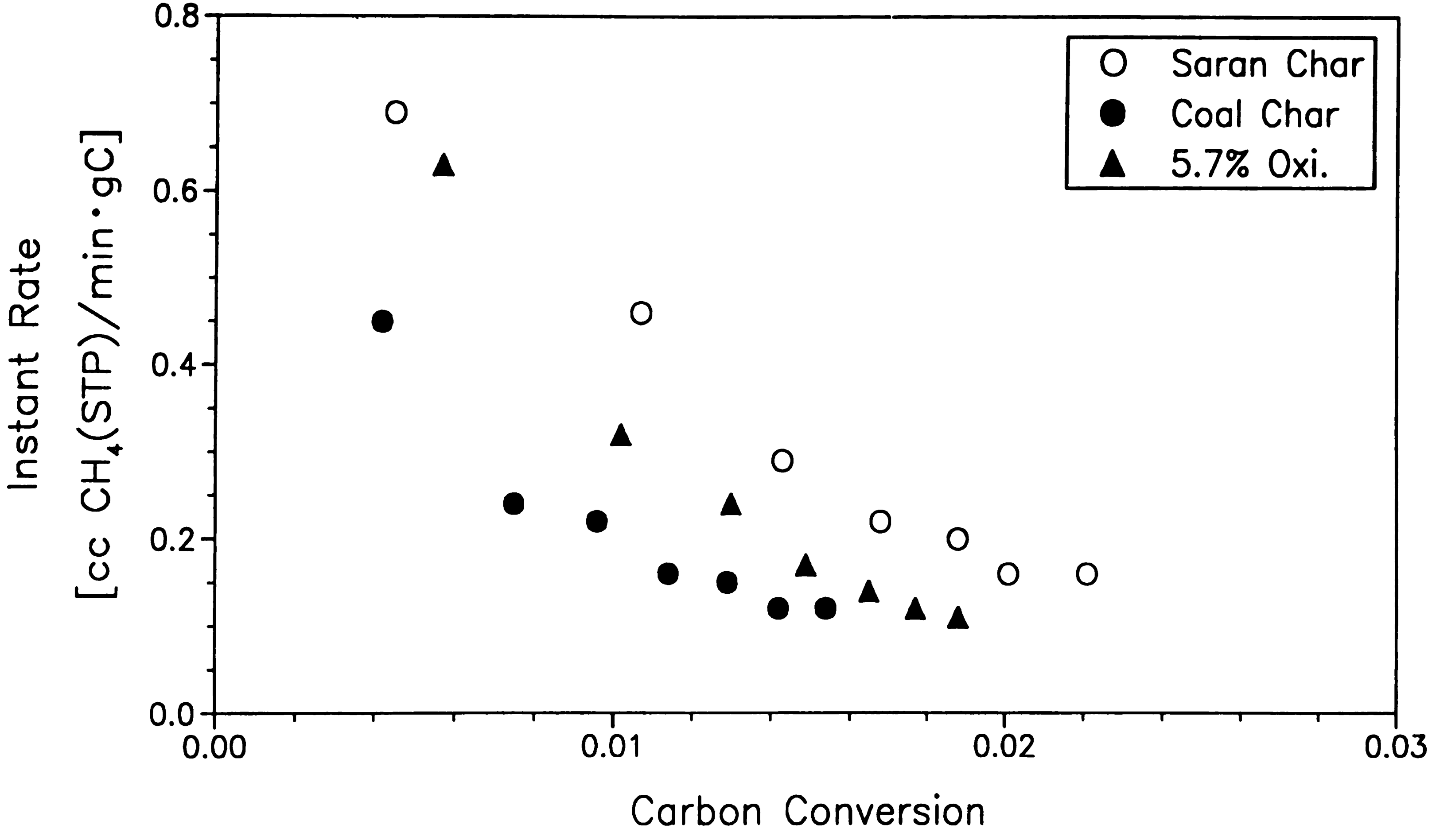

Figure 19: Hydrogasification of Saran, Coal, and Pre-Oxidized (375°C) Coal Char at 600°C and 500 psi H_2

and lost 5.7 wt% upon partial combustion. The Saran char reactivity is about twice that of the coal char, while the pre-oxidized coal char has a rate that is slightly higher than the coal char initially. The reactivity of all chars decreases rapidly in the same way it decreases during hydrogasification at 725°C.

3.7. HYDROGEN PRETREATMENT

Dissociative adsorption of hydrogen may poison the reaction of hydrogen with chars. Hydrogasification at reduced temperature and pressure and subsequent effects on hydrogasification rate at 725°C and 500 psig are shown in Figures 20 and 21. The duration of the pretreatment was 2.25 hours for all samples. This was the same length of time of all hydrogasifications in these figures, except the base case. The pretreatment shown in Figure 20 was initial gasification at 725°C and 10 psi hydrogen. The rate during the pretreatment conditions was much lower than that of the base case, while the rate after standard gasification conditions were imposed appears to have become greater than that of the base case. The first pretreatment shown in Figure 21 was gasification of coal char at 600°C under 50 psi hydrogen, which did not produce a rate high enough to accurately record. The gasification

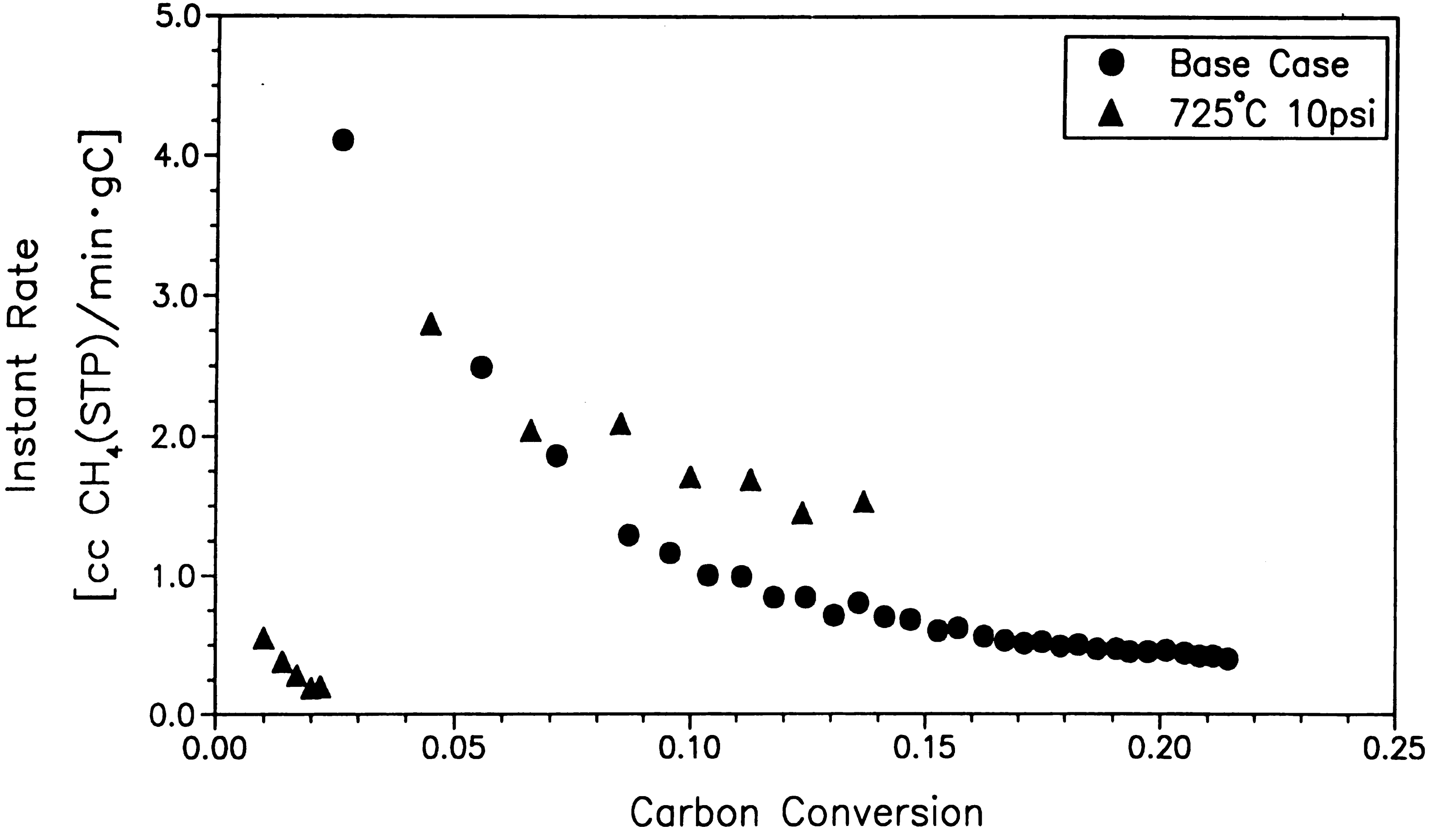

Figure 20: Effect of 725°C Hydrogen Pretreatment on Hydrogasification of Coal Char

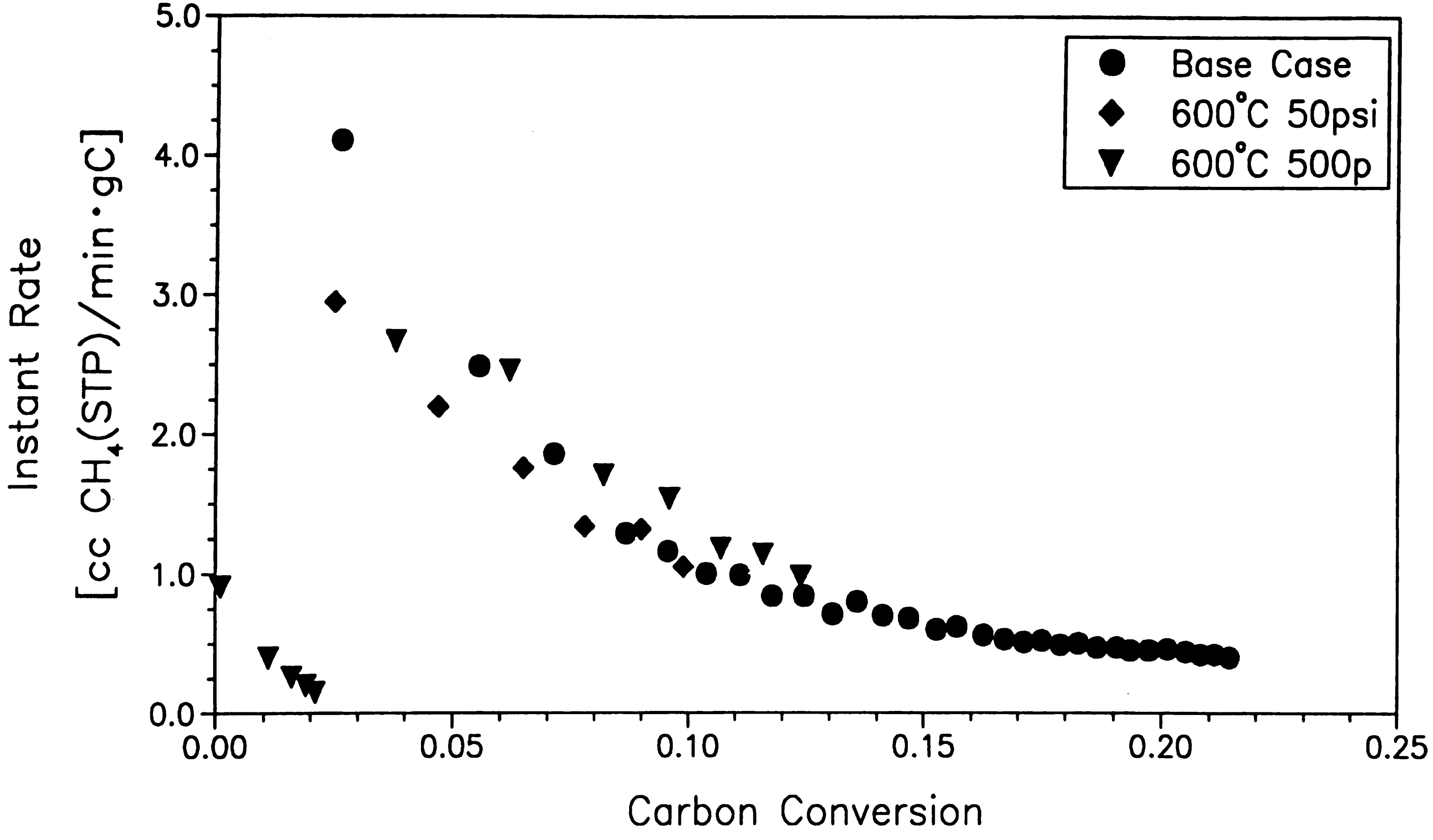

Figure 21: Effect of 600°C Hydrogen Pretreatments on Hydrogasification of Coal Char

rate of this sample after pretreatment was slightly lower than the base case. The final pretreatment was an initial gasification at 600°C and 500 psi hydrogen, which gave a low but measurable rate. Upon exposure to normal gasification conditions, which were 725°C and 500 psi hydrogen for this study, the sample reacted at a rate that was close to that of the base case. Overall, the effects of the hydrogen pretreatments on hydrogasification rate were minor.

3.8. CATALYST ADDITION

3.8.1. CATALYZED BASE CASES

Figures 22A and 22B show the effect on hydrogasification rate of loading 10 wt% potassium carbonate onto the various chars. The catalyzed coal char reacted at a rate almost double that of the uncatalyzed coal char, and the rate decayed in a similar manner after 8 hours of gasification. The catalyzed Saran char and catalyzed demineralized coal char began hydrogasification at a rate slightly higher than that of the catalyzed coal char, but their rates did not decay with time. The catalyzed Saran char reacted at a steadily increasing rate until about 75% carbon conversion, where the rate dropped

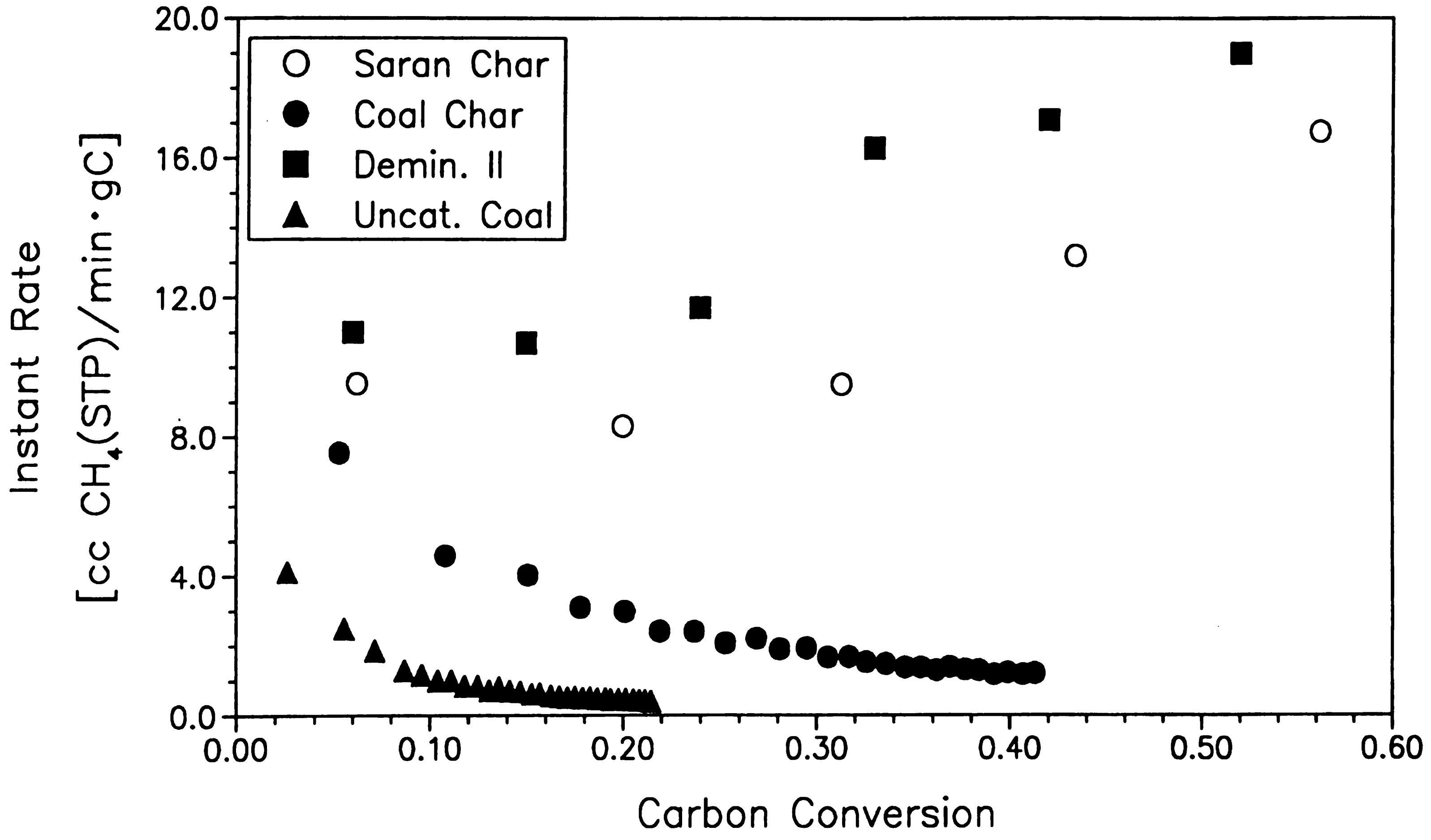

Figure 22A: Effect of K_2CO_3 Catalyst on Hydrogasification of Various Chars

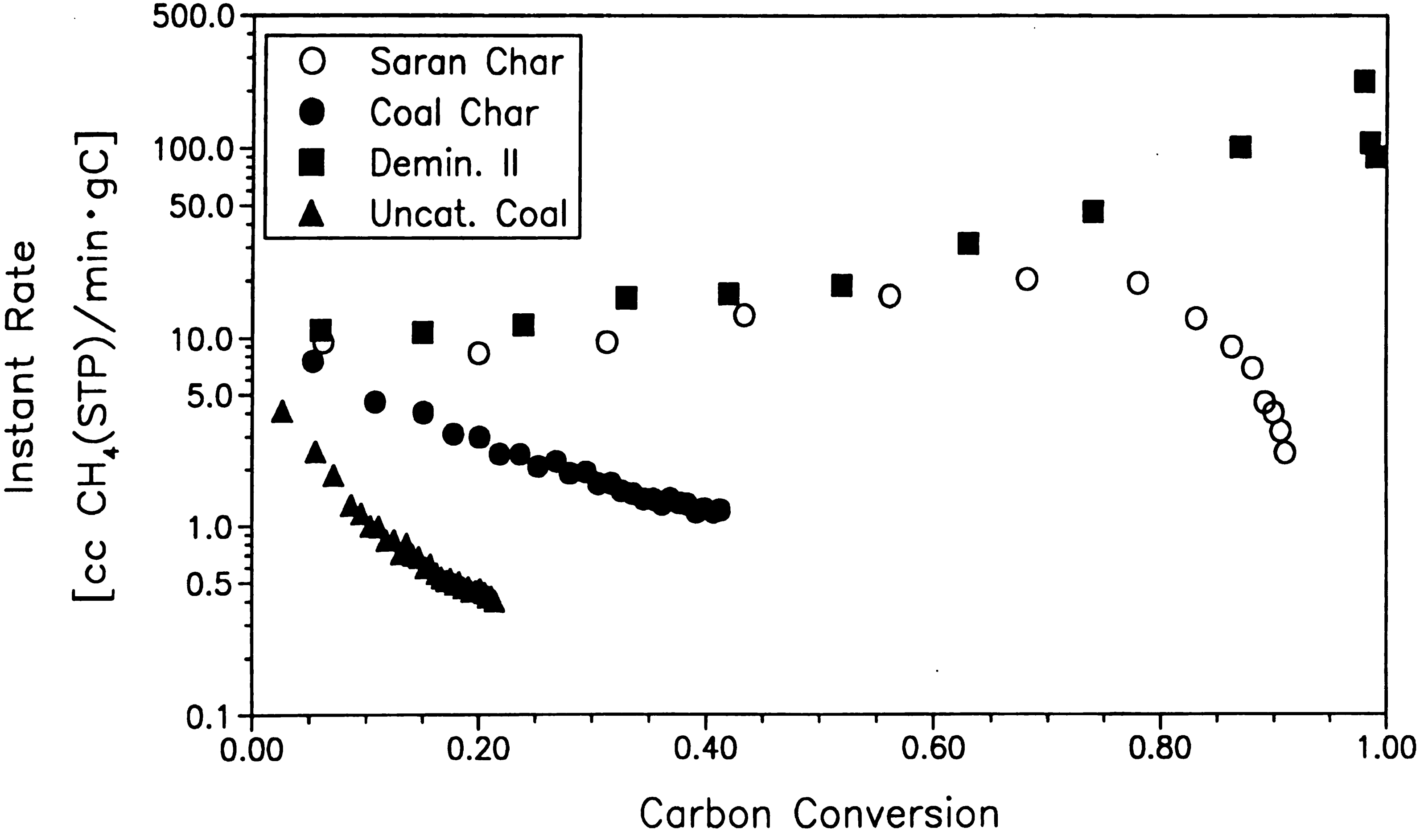

Figure 22B: Effect of K_2CO_3 Catalyst on Hydrogasification of Various Chars abruptly. After 4 hours of hydrogasification, the catalyzed saran char was over 90% converted. The catalyzed demineralized coal char reacted at a rate that increased rapidly until near completion after 2 hours, and had a higher rate than the Saran char.

3.8.2. PREOXIDATION OF CATALYZED CHARS

The effect on hydrogasification rate of preoxidizing coal chars before catalyst impregnation is shown in Figure 23. The first char had not been oxidized, while the second had been oxidized in air at 375°C and lost 5.7 wt% upon partial combustion. The third char had been oxidized in air at 725°C and lost 3.7 wt% upon partial combustion. Both preoxidized-catalyzed chars were gasified for 2.25 hours. No rate enhancement is evident over that of the catalyzed coal char base case.

3.8.3. INTERMITTENT OXIDATION OF CATALYZED CHARS

The effect on hydrogasification rate of intermittent oxidation of various catalyzed chars is shown in Figure 24. The catalyzed Saran char was oxidized at 375°C in air after 2.25 hours of hydrogasification. The rate after intermittent oxidation decreased to less than one third that of the catalyzed base case, but the rates did not

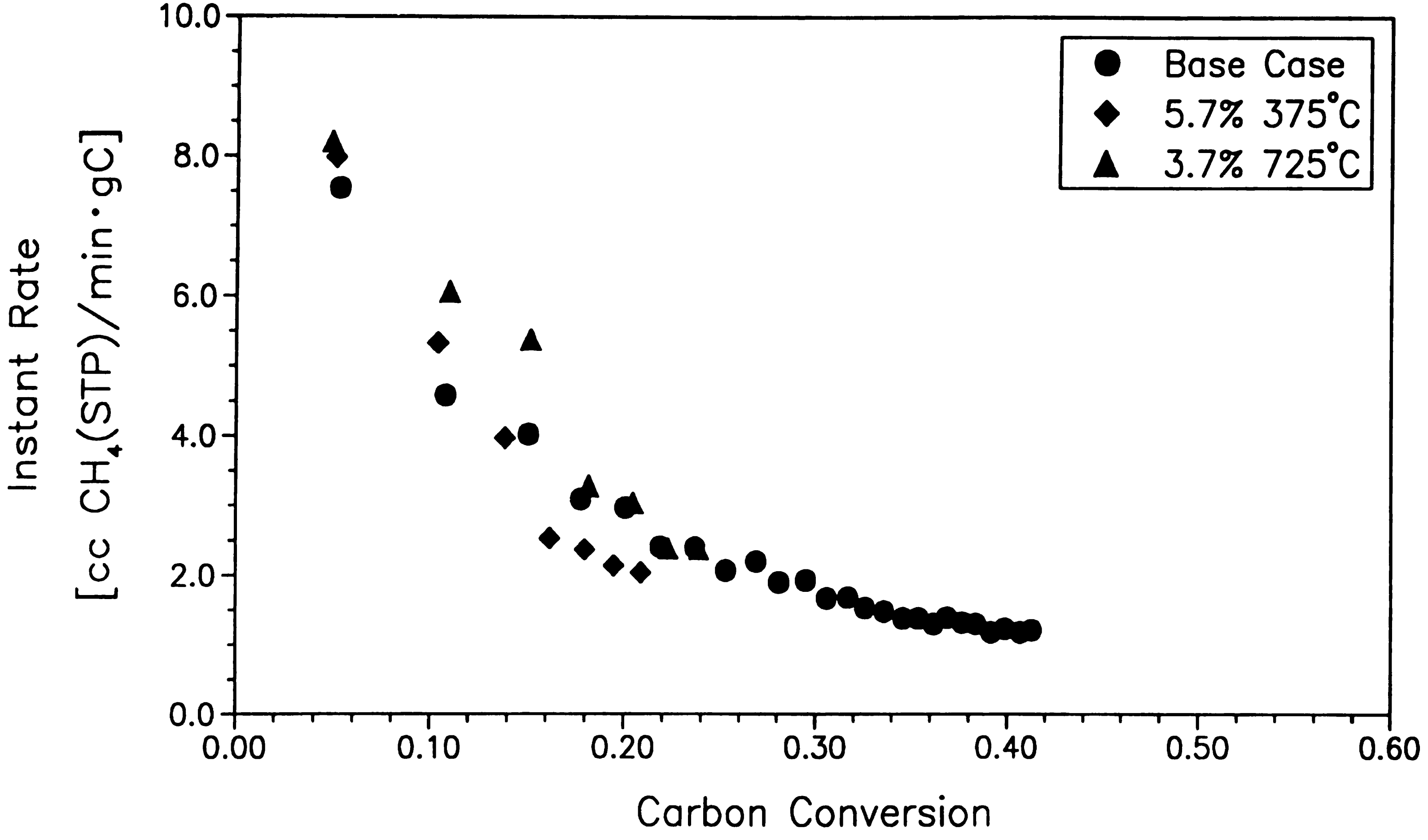

Figure 23: Effect of K_2CO_3 Catalyst on Hydrogasification of Pre–Oxidized Coal Chars

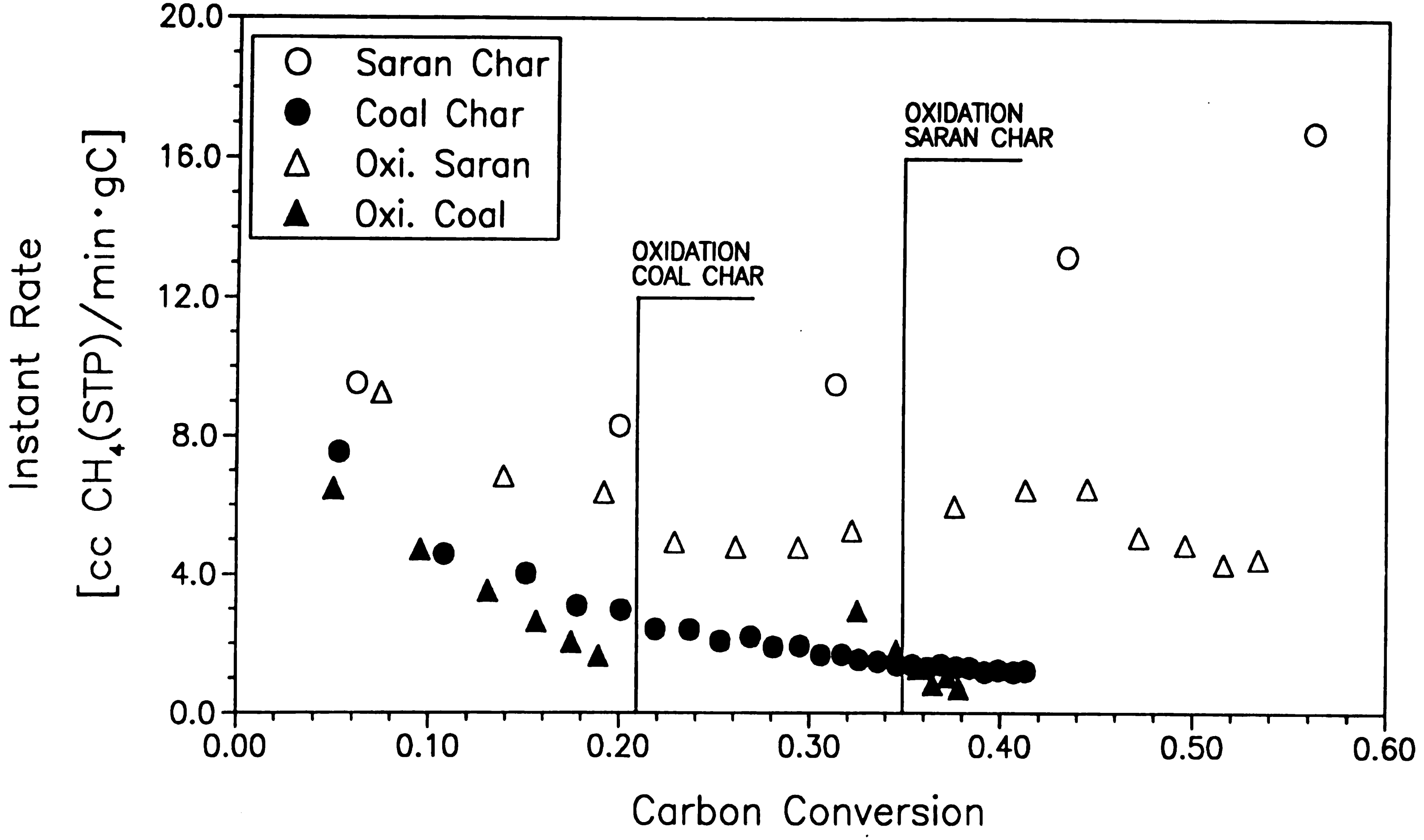

Figure 24: Effect of Intermittent Oxidation at 375°C on Hydrogasification of K_2CO_3 Catalyzed Chars

match up well before the intermittent oxidation. The catalyzed coal char was oxidized at 375°C in air after 2.25 hours of hydrogasification. It lost about 10 wt% during partial combustion, which caused a large gap between data points. During the second gasification it started at a rate higher than that of the catalyzed base case coal char, but dropped below it after 3% carbon conversion. As with the catalyzed Saran char, the catalyzed coal char reaction rates did not match up well with each other before the intermittent oxidation.

Chapter 4

Discussion

4.1. GENERAL OBSERVATIONS

4.1.1. TEMPERATURE EFFECTS

It has been shown that the conditions chosen for hydrogasification in this investigation result in kinetic and not mass transfer rate limitations, with the exception of the first 2-3% carbon conversion. The activation energy calculated from the Arrhenius plot in Figure 3 is consistent with those found in literature.[17,18] The temperature range in which diffusion limitations dominate, which will be above a certain threshold, is indicated by the section of the Arrhenius curve that has a slope which gives half the activation energy of the reaction. In this system, that transition occurs near 775°C. This is 50°C higher than the gasification temperature chosen for this investigation. An interesting phenomenon illustrated by the Arrhenius plot is the apparent decrease in rate from a gasification temperature of 775°C to 800°C. Hydrogasifications to produce these data points have been duplicated to ensure their validity. This unusual rate decrease with increased reaction temperature may due to the annealing effects at higher temperatures. Another possibility is the proportional increase in rates of reactions that are responsible for the consumption of active sites over the rates of reactions responsible for methane formation.

Gasification rates measured during runs with the newly designed sample mount are consistent with rates measured during runs with the original sample mount design. This demonstrates that mass transfer limitations are not taking place because of particle size, since larger sample particle sizes are required for the newly designed mount. A gasification run was made with the original mount containing a sample weight that was 40% of the usual starting weight to investigate the possibility of mass transfer limitations because of the sample bed depth. The rates curves are identical, indicating diffusion limitations do not occur because of the bed depth either.

4.1.2. TOTAL SURFACE AREA

Figure 25 shows total surface area changing very little with carbon conversion for Saran char and coal char. Since the hydrogasification rate changes significantly within the 0-20% conversion range, it appears that rate is only a very weak function of total surface area. Analysis of Figure 26, however, indicates that this may not be the case in conversions above 20%. The rate per unit total surface area appears to reach a constant level for coal at about 15%, and may be leveling off for Saran char at about 25% conversion. The possibility of a mechanism in which at least two different modes of hydrogasification occur is supported if the rate is not a function of total surface area for the first 15-25% carbon conversion, but it is for the rest of the reaction.

4.1.3. ACTIVE SURFACE AREA

Figure 27 shows the active surface area of Saran char and coal char as a function of carbon conversion in hydrogasification. The coal char results are erratic, with the last data point being unusually high. Later measurements of just the coal ash after exposure to hydrogasification conditions revealed an active surface

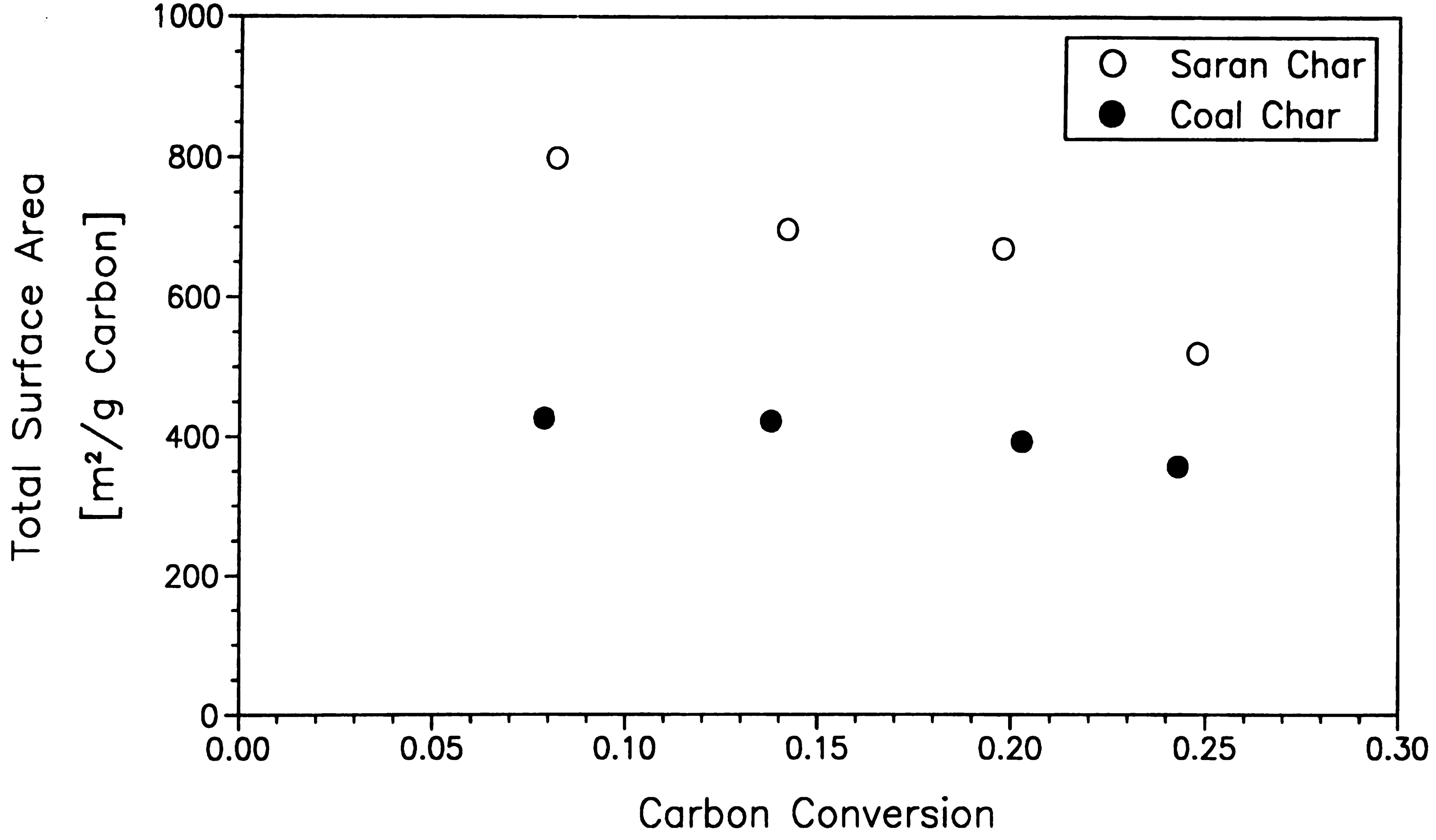

Figure 25: Total Surface Area of Chars at Various % Conv. in Hydrogasification

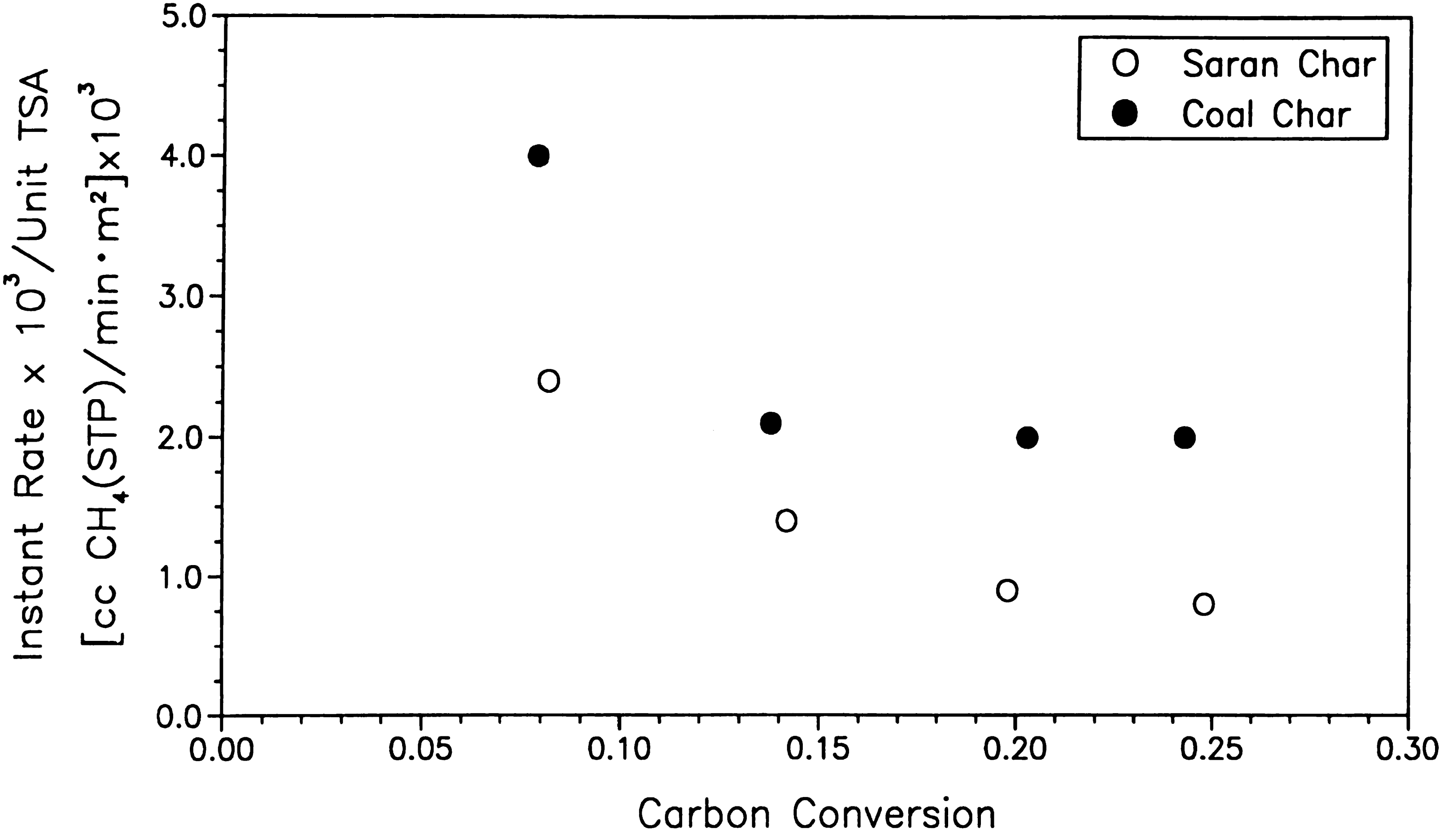

Figure 26: Instant Rate x 10^3/Unit Total Surface Area for Various %Conversion in Hydrogasification of Chars

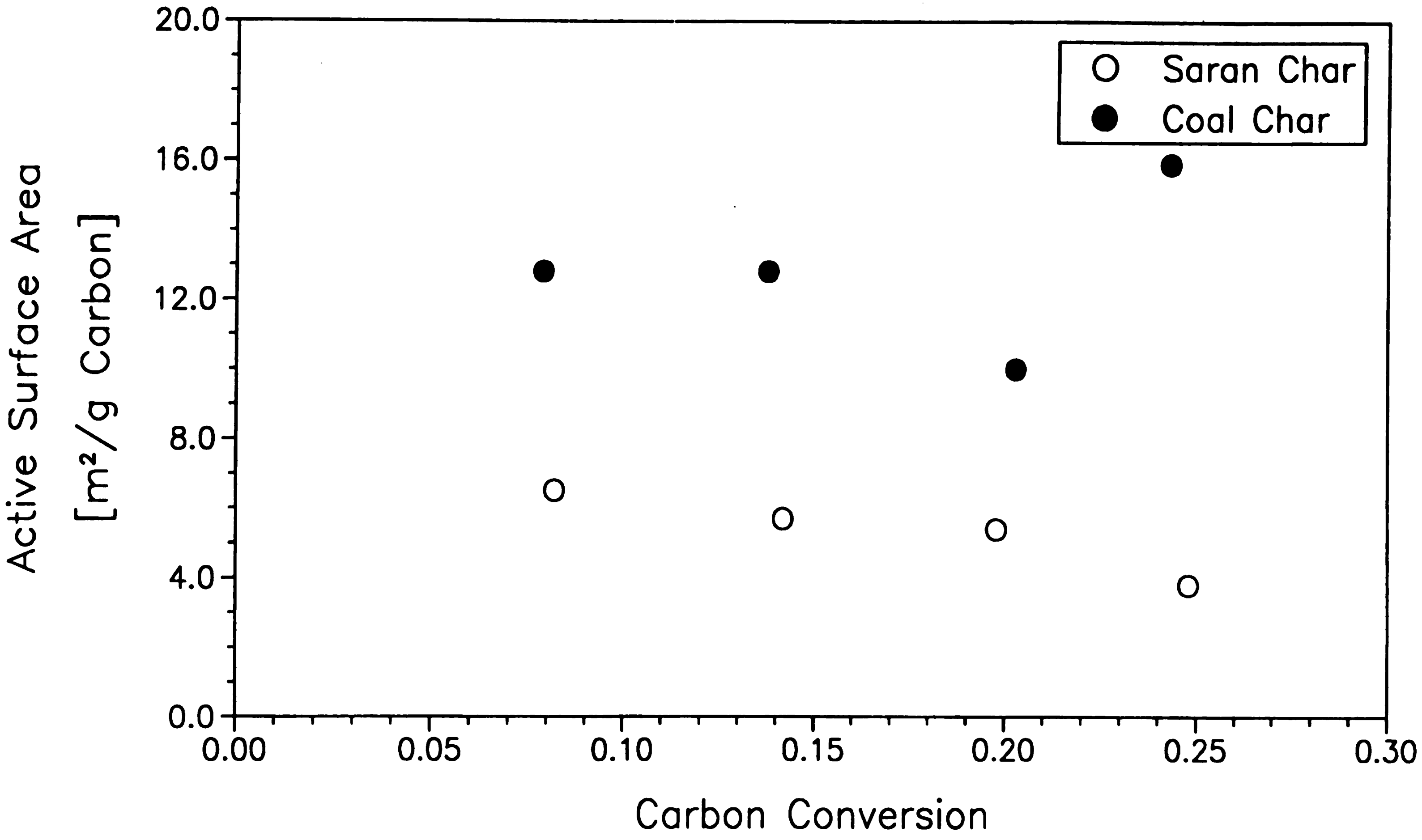

Figure 27: Active Surface Area of Chars at Various % Conv. in Hydrogasification

area of $74 m^2/g$, which is very high relative to the coal. This cannot be compensated for in the active surface area calculations because it is not known exactly how much of the ash is exposed at various stages during gasification. Thus, measurement of active surface area using oxygen chemisorption is not feasible for hydrogasified coal char.

The general trend of the Saran char data is similar to that of the total surface area data. Figure 28 shows the rate per unit active surface area as a function of carbon conversion. The Saran char data indicate a possible leveling off of rate per unit active surface area in a manner similar to rate per unit total surface area in Figure 27. This may also support a multi-stage mechanism.

It is apparent that the method used for active surface area measurement in this investigation is not indicative of the active surface area that is important during hydrogasification. Table 4.1 shows the active surface area of two parallel runs of intermittently oxidized Saran char. The values given describe char properties at the end of each stage. According to the values given, the active surface area is lower at the beginning of a hydrogasification stage than at the end of that stage, and the active surface area is higher at the beginning of an oxidation stage than at the end of that stage. This is the inverse of what would be expected. The active surface area should decrease with

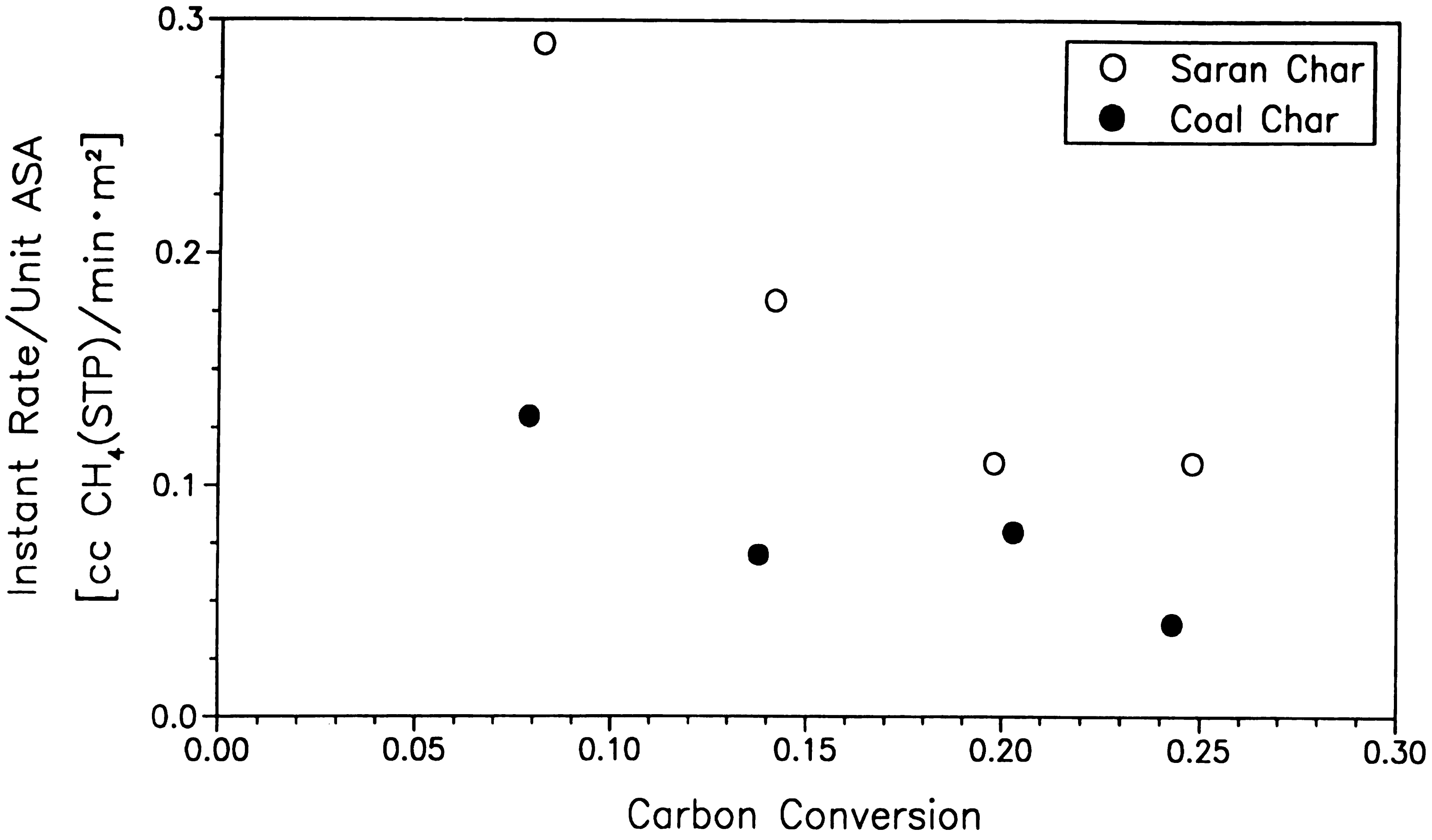

Figure 28: Instant Rate/Unit Active Surface Area for Various %Conversion in Hydrogasification of Chars

Table 4.1: ACTIVE SURFACE AREA OF INTERMITTENTLY OXIDIZED SARAN CHAR - TWO DIFFERENT RUNS[1]

Stages During Experiment	% Conversion		ASA (m2/g C)[115]	
	Run A	Run B	Run A	Run B
Starting:	00.00	00.00	4.0	4.0
Gasification #1:[2]	14.5	14.7	7.8	NA
Oxidation #1:[3]	0.32	-2.51	4.9	4.3
Gasification #2:	19.9	21.0	6.1	>5.1
Oxidation #2:	-1.24	-1.75	4.0	3.4
Gasification #3:	NA	24.7	NA	6.6

1. Values are reported at the end of each stage of treatment.
2. All gasifications are 2.25 hours at 725°C in 500 psi H_2.
3. All oxidations are 1 hour at 375°C in stagnant air.

hydrogasification since the rate decreases, because rate is thought to be a function of surface oxygen group concentration. The active surface area should increase after oxidation, since oxidation fixes oxygen functional groups on the char surface. Explanations for this include the possibility of oxygen binding more strongly to the highly reduced char surface after hydrogasification, or reaction of oxygen with surface hydrogen to produce water after hydrogasification.

4.1.4. OXIDATION EFFECTS

It is evident that preoxidation via partial combustion in air does not enhance the hydrogasification rate of pyrolyzed chars at 725°C. However, it does enhance the reaction rate of chars that have been pyrolyzed, then outgassed. Table 4.2 shows surface analyses of most of the chars used in this investigation. It is clear that oxygen is being fixed onto the char surfaces during partial combustion in air because the O/C ratio increases in all but one case. The O/C ratio for the outgassed samples is lower than the samples that have not been outgassed. The decreased Saran char gasification rate following outgassing is due to the decreased surface oxygen concentration and not the collapse of pore structure, since the total surface area increases slightly

Table 4.2: SURFACE ANALYSIS OF VARIOUS CHARS[113]

Sample	TSA[1]	ASA[2]	O/C Ratio[3]	ΔpH[4]
SARAN CHAR	816	4.0	0.066	-0.44
Oxidized 375°C, 3.1% Burnoff	815	6.1	0.108	-2.54
Oxidized 375°C, 7.7% Burnoff	876	9.9	0.152	-3.38
Outgassed 1000°C	870	1.5	0.043	+0.55
Outgassed 1000°C, then Oxidized 375°C, 0.4% Burnoff	762	2.3	0.080	-2.42
Gasified 725°C	754	NA	0.018	+2.70
COAL CHAR	274	4.0	0.062	+4.55
Oxidized 375°C, 0.1% Burnoff	218	NA	0.052	+0.82
Oxidized 375°C, 5.7% Burnoff	195	NA	0.128	-1.66
Oxidized 725°C, 3.7% Burnoff	NA	NA	0.093	+2.88
Outgassed 1000°C	7	0.6	0.012	+3.71
Outgassed 1000°C, then Oxidized 375°C, 0.5% Burnoff	87	0.9	0.100	+2.92
Outgassed 725°C	NA	NA	NA	+4.16
Outgassed 725°C, O_2 Chemsorbed	NA	NA	NA	+3.88
Gasified 725°C	313	NA	0.052	+3.46
Gasified 725°C, Oxidized 375oC	316	6.3	NA	+0.91
DEMIN. I COAL CHAR	322	1.3	0.066	-0.63
Oxidized 375°C, 2.3% Burnoff	354	6.9	0.094	-1.29
Oxidized 375°C, 6.3% Burnoff	376	6.7	0.092	-2.75
Gasified 725°C	363	NA	NA	+3.17

1. Units in m^2/g Carbon

2. Units in m^2/g Carbon

3. Oxygen in the form of metal oxides is not included in this ratio (SnO_2, Al_2O_3, SiO_2, et.al.).

4. Units are difference in pH between a 0.1 M KCl solution containing the char and a standard 0.1 M KCl solution, both heat treated under reflux (ASTM method D3838-80).

both heat treated under reflux (ASTM method D3838-80).

during outgassing. The coal char loses much more surface oxygen and total surface area upon outgassing. There may be a contribution of both phenomena to the lowering of the hydrogasification rate of coal char because less surface oxygen means fewer functional groups, and collapse of the pore structure may cause blockage of the reactant gas from these groups.

There does seem to be some enhancement in rate for gasifications performed on non-outgassed coal chars at 600°C during the first 2% carbon conversion, as seen in Figure 19. This rate enhancement does not appear to occur at 725°C because steady state conditions are not reached until about 5% conversion, after the rate enhancement has already died out. Figures 29A, 29B, 30A, and 30B show the rate data at 600°C normalized to 725°C via activation energy for Saran char, coal char, and preoxidized coal char. The highly deactivating nature of the hydrogasification reaction is very clearly illustrated.

Intermittent oxidation via partial combustion in air does produce a noticeable hydrogasification rate enhancement at 725°C. The rate after an intermittent oxidation never reaches the rate measured at the beginning of the first hydrogasification and only lasts for about 5% carbon conversion before it decays back to the base level. This seems to indicate that it takes roughly 5% carbon conversion to consume the additional active sites formed

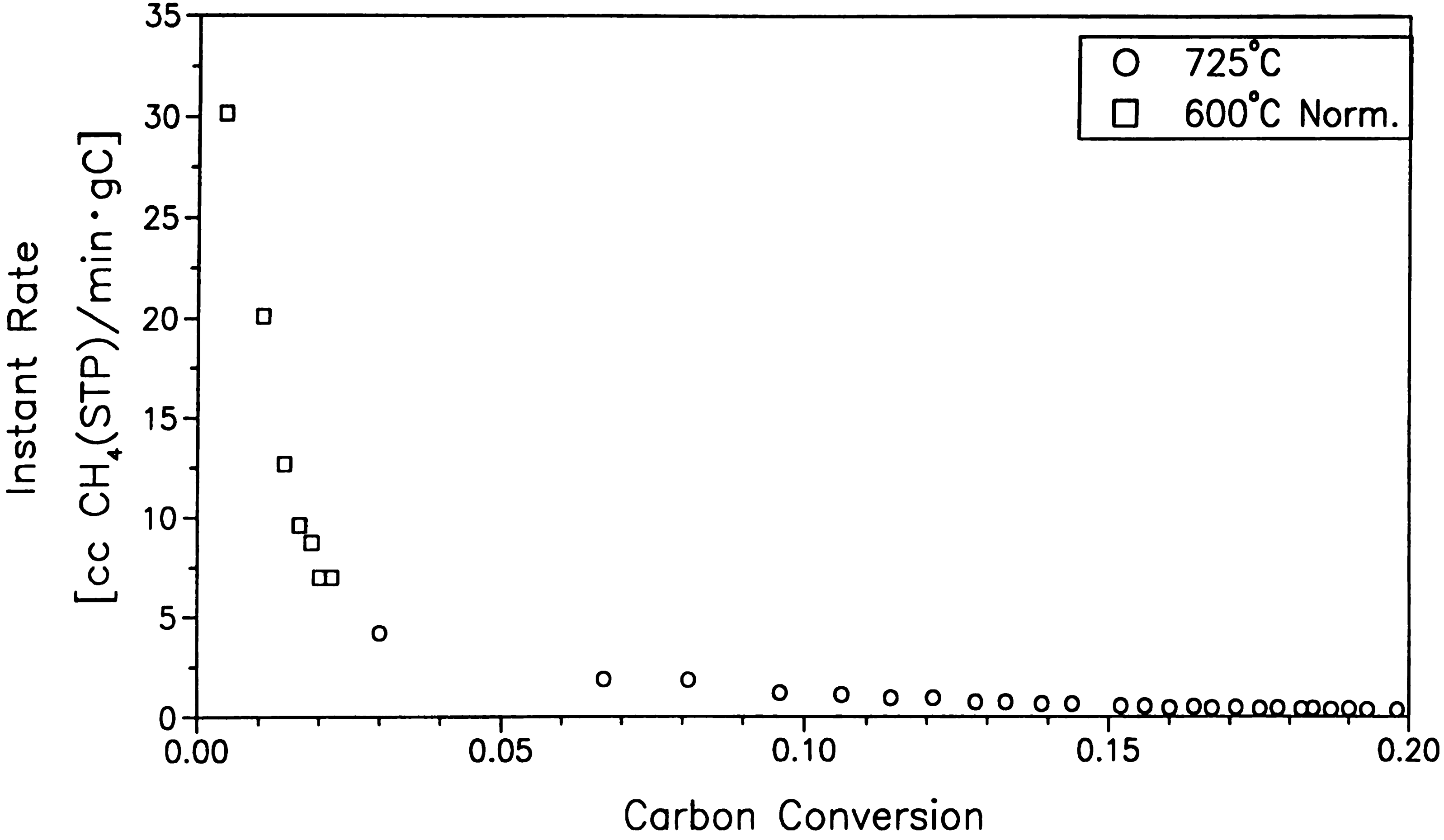

Figure 29A: Hydrogasification of Saran Char – Rate Normalized from 600°C to 725°C via Activation Energy

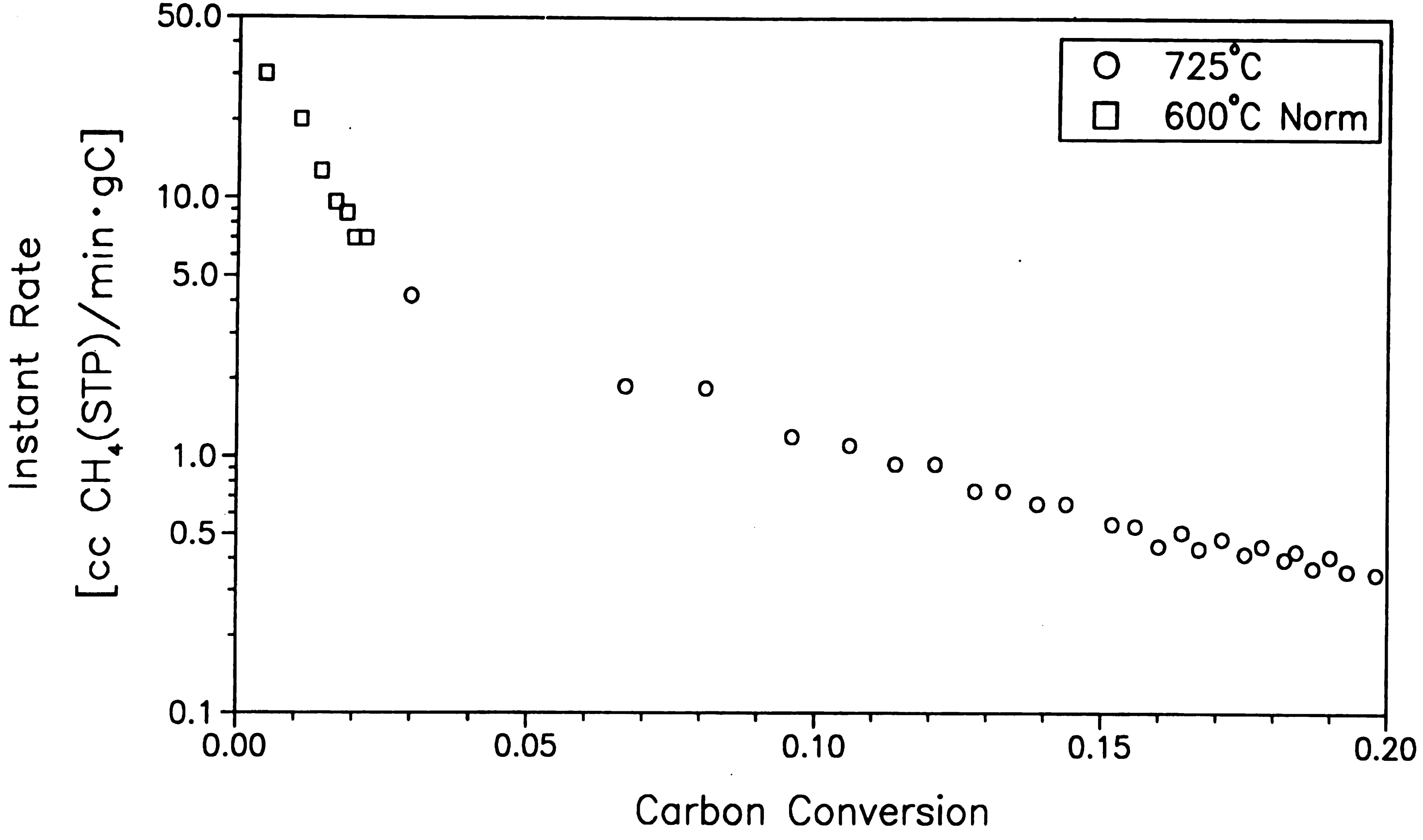

Figure 29B: Hydrogasification of Saran Char – Rate Normalized from 600°C to 725°C via Activation Energy

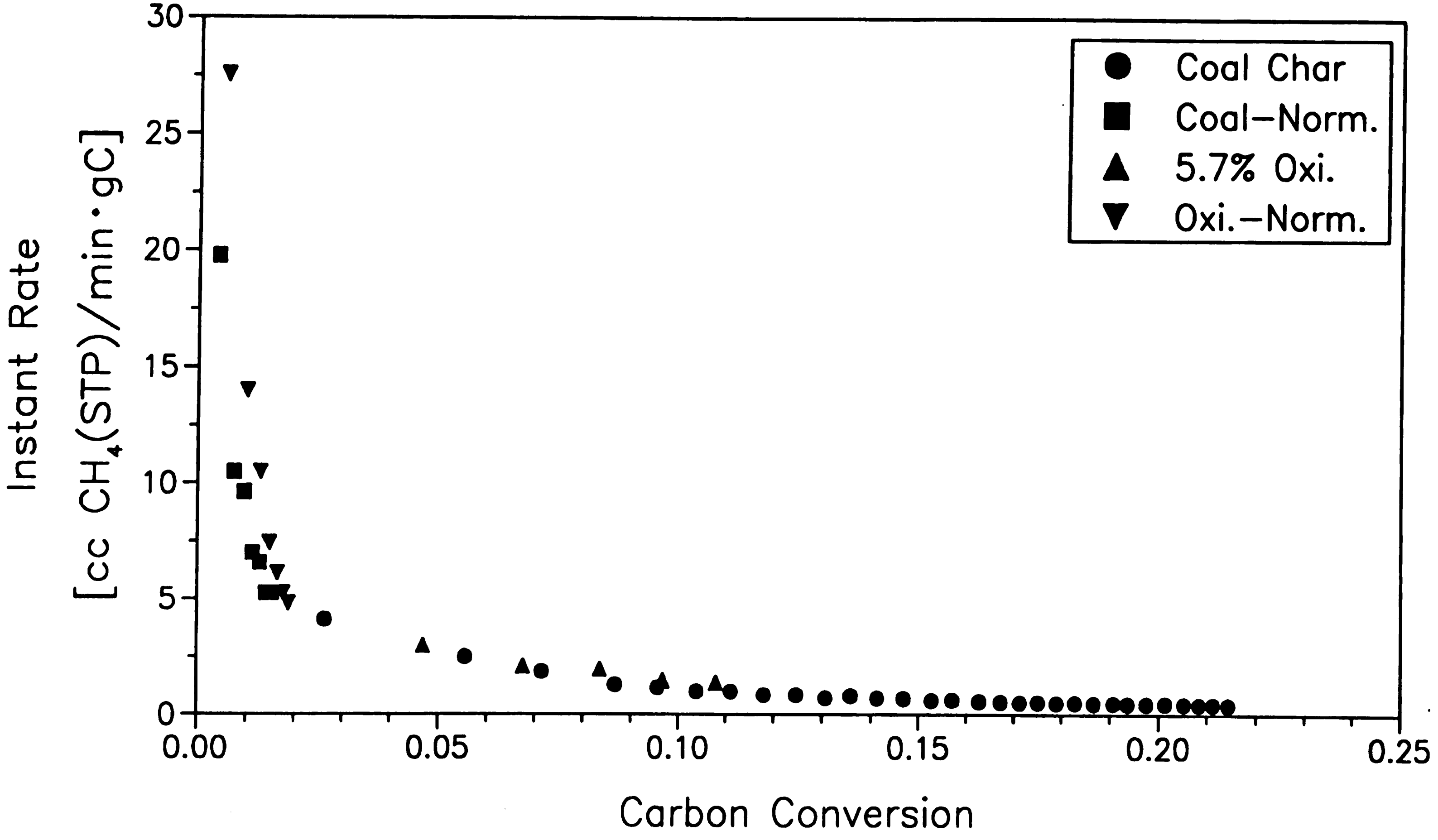

Figure 30A: Hydrogasification of Coal Chars – Rate Normalized from 600°C to 725°C via Activation Energy

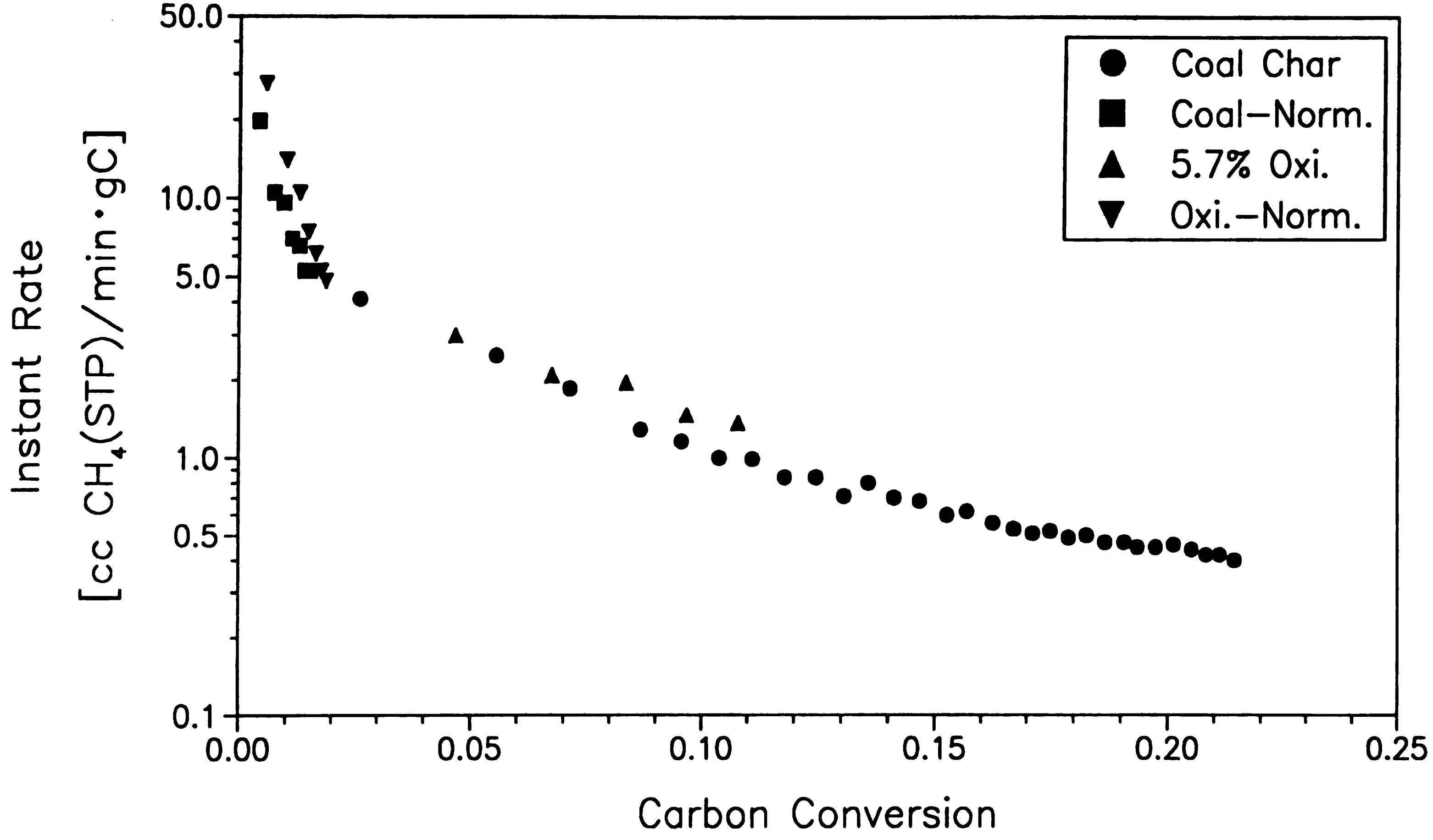

Figure 30B: Hydrogasification of Coal Chars – Rate Normalized from 600°C to 725°C via Activation Energy during oxidation. The intermittent oxidation performed on coal char at 725°C produced an enhancement comparable to the intermittent oxidations at 375°C. This finding suggests that the nature of the functional groups may not be as important a factor as previously thought in determining the hydrogasification rate of chars, since acidic groups would be formed at 375°C and basic groups at 725°C.

4.1.5. CATALYST EFFECTS

It has been shown in this study that coal ash does not catalyze or poison coal char that has not been treated with potassium carbonate. It has also been shown that potassium carbonate greatly catalyzes the hydrogasification of chars that contain very little or no mineral matter. In the latter stages of gasification, there may be a rate increase up to three orders of magnitude for Saran char and four orders of magnitude for demineralized coal char. Coal ash, which contains sulfur and aluminosilicates, strongly poisons the catalyst. Even though the gasification rate of the catalyzed coal char is twice the rate of the uncatalyzed coal char, the catalyzed coal char rate does not increase with conversion like the demineralized catalyzed coal char and the Saran char.

Preoxidation has no apparent effect on the catalyzed char reaction rate at 725°C, which is the same result found for uncatalyzed chars. Intermittent oxidation of the catalyzed coal char produces a mild rate enhancement that decays quickly. This result is also similar to that observed for uncatalyzed chars.

4.2. MECHANISTIC CONSIDERATIONS

A multi-stage reaction and the concept of creation of active sites by oxygen functional group desorption are both supported by this investigation. Hydrogen inhibition is not observed with any of the hydrogen pretreatments, indicating that dissociative hydrogen poisoning may not be the cause of the sharp hydrogasification rate decay with sample conversion. Previous studies have proposed a variety of two-stage reactions for char hydrogasification.[8,25,26] The best explanation for the phenomena observed in this study is a three-stage reaction for hydrogasification.

4.2.1. PROPOSED MODEL

The dominant reaction during the first stage is the rapid hydrogasification of amorphous "secondary" carbons that are partially saturated with hydrogen, yet are probably not saturated with chemical bonds. One category of amorphous carbons is high molecular weight compounds that are not chemically bound to the char surface, but remain in char because they are not volatile enough to enter the gas phase during pyrolysis. The other category of amorphous carbons includes carbon structures that are partially saturated with hydrogen and chemically bound to the char base structure. If some of these groups gasify via active sites, the sites may propagate to the base structure during gasification.

The second stage involves hydrogasification of base char carbons via active sites formed by oxygen functional group desorption, and the preferential hydrogasification of carbons located on the armchair edges of aromatic planes. There is probably a great deal of overlap between these two categories of carbon. It is also possible that active sites propagate to the base char structure from the chemically bound amorphous carbons and contribute to the second stage gasification reaction.

Rate during the third stage of hydrogasification is low because the carbons that react are primarily those on the relatively unreactive zig-zag edges of the aromatic planes. There are very few armchair edges because they have been consumed during the second stage. The only sources of surface oxygen functional groups are oxygen migration to the char surface or the uncovering of oxygen from the bulk char by removal of carbons. Because the char surface has become very non-reactive and homogeneous, the reaction rate becomes proportional to the total surface area.

Preoxidation does not increase or decrease the hydrogasification rate within the conversion range measurable by the equipment used in this investigation because two opposing effects roughly cancel each other out with respect to the char's reactivity with hydrogen. One force at work is a decrease in the ratio of amorphous carbons to those of the basal aromatic planes by somewhat preferential oxygen attack, and the other is the creation of more oxygen functional groups on the aromatic base structure.

Intermittent oxidation increases the hydrogasification rate, and brings the reaction from the third stage back to the second. No amorphous carbon structures are formed upon intermittent oxidation, so the rate will not be as high as that which is observed initially. Oxygen functional groups are formed on the char surface, which create active sites upon desorption. Oxidation also increases the ratio of armchair carbons to zig-zag carbons. This happens because oxygen, unlike hydrogen, does not preferentially react with either type of edge carbon, thus leaving both present following oxidation. Since armchair carbons are more reactive toward hydrogen than zig-zag carbons, their ratio is an important parameter in determining the reactivity of a char.

4.2.2. SUPPORTING OBSERVATIONS

There are several observations that support the proposed three-stage hydrogasification reaction in this study. Dissociative hydrogen poisoning and rate dependence upon pore structure within the first 20% carbon conversion have not been included in the proposed model. This is because they have been shown not to affect rate or correlate to rate within the first 20% carbon conversion respectively.

Initial rate decreases rapidly with conversion and cannot be matched with the intermittent treatments used in this investigation. This indicates that there may be more than one reaction stage present. Further, it supports the claim that there is a small amount of highly reactive char on the sample surface, which is consumed during the first 5% carbon conversion. If the high initial rate was due only to the number of oxygen functional groups on the char surface, then intermittent oxidation would restore the functional groups and increase the hydrogasification rate to its original value, but this is not observed.

Preoxidation neither increases nor decreases the initial reaction rate as can be detected by the equipment used in this investigation. The highly volatile material contained in the starting coal is drawn out of the bulk material upon pyrolysis, leaving pores. Most of the volatile material is carried away in the gas phase, but some carbonizes on the char surface. Because of the way amorphous carbon structures are formed, it would seem likely that most of the char total surface area would initially be coated with them, so gases would have to react with amorphous carbon structures before they could react with carbons of the basal aromatic planes. From a physical standpoint, it is likely that any reactant gas would preferentially attack the amorphous carbons. This proposed idea is supported by the facts that preoxidation has been shown to increase the concentration of surface functional groups, but it does not enhance the initial hydrogasification rate.

This study shows that hydrogasification rate declines rapidly and appears to become constant with total surface area after about 20% carbon conversion. The O/C ratio is low, and etch pit analysis performed by other researchers shows the predominance of zig-zag carbon configurations.[29-32] If oxygen functional groups are uniformly distributed throughout the basal carbon matrix, they should be uncovered by the consumption of overlying carbons at a fairly uniform rate and be distributed fairly evenly over the char surface. This means a roughly constant ratio of total surface area to active surface area caused by desorption of freshly uncovered oxygen groups. Since the hydrogasification rate is thought to be proportional to the active surface area, it should be proportional to the total surface area during the third gasification stage. Observations in this study appear to indicate constant rate per unit total surface area during the third stage of hydrogasification.

Intermittent oxidation has been shown to increase the O/C ratio in this study. Other researchers have shown oxygen to form round etch pits [29,32]. As the oxygen attacks the zig-zag edges, it must leave both zig-zag and armchair edges behind. This must increase the ratio of armchair to zig-zag carbons and partially cover the edges with oxygen functional groups, supporting the claim that partial oxidation serves as a source for regeneration of these configurations after they have been destroyed during hydrogasification.

CHAPTER 5

CONCLUSIONS AND RECOMMENDATIONS

5.1. CONCLUSIONS

The major objective of this investigation was to gain a more fundamental understanding of the hydrogasification reaction, and to determine ways to increase the reaction rate based upon this knowledge. In order to ensure kinetic and not mass transfer limitations, the proper reaction temperature, 725°C, was established. It was also determined that mass transfer limitations were not occurring due to particle size or sample bed depth.

Hydrogasification rates of Saran char and coal char were shown to decay rapidly with conversion, and were similar in magnitude. Rate for the first 2-3% carbon conversion could not be measured at the established reaction temperature, but the sharp rate decay during the rest of the reaction was evident. The sharp rate decay was shown much more clearly by normalizing hydrogasification rates measured at 600°C for the first 2-

3% carbon conversion. For uncatalyzed hydrogasification, initial rate decays by a factor of five after 10-15% carbon conversion, and a factor of ten after 20-25% carbon conversion. Total surface area was found not to be a char characteristic that correlates with hydrogasification rate within the first 15-25% carbon conversion, but may correlate well at conversions greater than this. This indicates that the chemical nature of the char surface is of fundamental importance in determining hydrogasification rate.

One focus of this investigation was to study hydrogen inhibition. Several hydrogen pretreatments were done at conditions less severe than those chosen for standard gasification during this experimentation, so hydrogasification rates would be low. Some pretreatments were performed at either 725°C or 500 psi H_2, but none resulted in rate inhibition at standard gasification conditions.

Another focus of this investigation was to study the role of oxygen in hydrogasification. It was found that partial combustion in air increases the char surface oxygen concentration. These surface oxygen functional groups desorb during heatup to hydrogasification conditions and leave active sites where the reaction takes place. Partial combustion in air increased the subsequent hydrogasification rate of chars that had been outgassed or previously gasified in hydrogen, but did not increase the reaction rate of fresh chars. The hydrogasification rate of chars that had been oxidized following outgassing or hydrogasification was not restored to that shown initially by a fresh char. Reaction rate following outgassing was an order of magnitude lower than that of fresh char.

An attempt was made to accurately measure the concentration of active sites on char surfaces in this investigation. Coal ash was shown to have a very high active surface area, which interfered with measurement. The active surface area measurements for intermittently oxidized Saran char were the opposite of what they should have been. They showed a higher active surface area following hydrogasification, and a lower active surface area following intermittent oxidation. The opposite would be expected, because intermittent oxidation has been shown to increase the surface oxygen content and the hydrogasification rate. A new method must be devised to accurately measure char active surface areas.

The final focus of this investigation was to study the poisoning of the reaction by coal ash. It was found to neither poison nor catalyze the coal char that had not been treated with potassium carbonate. The hydrogasification rates of all chars used in this investigation were catalyzed by potassium carbonate, however it was found that coal ash greatly poisons this catalyst. Catalyzed Saran char and catalyzed demineralized coal char both had rate curves that started 2-3 times higher than the uncatalyzed chars and increased with conversion. The catalyzed coal char started at a rate that was about twice the uncatalyzed rates, and had a rate decay pattern similar to that of the uncatalyzed chars.

This set of observations supports a hydrogasification reaction that is composed of three stages in which each stage dominates during different ranges of carbon conversion. During the first stage, hydrogen reacts rapidly with the small amount of amorphous "secondary" carbon. This carbon is highly reactive because it is already partially saturated with hydrogen, but is not completely saturated with chemical bonds. The second stage involves hydrogasification of base char carbons via active sites formed by functional group desorption, and hydrogasification of carbons located on the armchair edges of the base char, which is composed mainly of randomly aligned graphite crystalites. Active sites formed during the first reaction stage may propagate to the base char and contribute to hydrogasification during the second stage. Rate during the third stage of hydrogasification is low because the carbons that react are primarily those on the relatively unreactive zig-zag edges of the aromatic planes. There are very few active sites or armchair edges left. During the third stage, reaction rate is roughly proportional to the char total surface area because the surface is relatively unreactive and homogeneous, and the only source of functional groups is oxygen trapped in the bulk char.

Preoxidation does not change initial char reactivity toward hydrogen within the measurable range of carbon conversion in this investigation because two effects roughly cancel each other out. One effect is the increase in the number of oxygen functional groups, which increases the overall char reactivity. The other effect is the somewhat preferential attack of the "secondary" carbons by oxygen, which decreases the overall char reactivity.

Intermittent oxidation increases char reactivities for two reasons. It increases the number of oxygen functional groups on the char surface, and it increases the ratio of the armchair carbons to zig-zag carbons. The rate increase from intermittent oxidation lasts for about 10% carbon conversion, after this the surface oxygen concentration has declined back to that of the bulk char and the carbons in the armchair configurations have all been gasified.

5.2. RECOMMENDATIONS

There are several tasks that can be done in the future to further the knowledge gained in this investigation. The main concept that needs more understanding is the cause of the sharp rate decay with sample conversion during hydrogasification. Several accomplishments would contribute to this understanding in the future. One would be to find a technique that measures the active surface area that is important during hydrogasification. A very useful parameter for characterizing char reactivity could result from the implementation of such a technique. Another task should be to modify the hydrogasification reactor and analysis equipment so better initial resolution of rate data is possible. This would aid in the investigation of initial rate phenomena tremendously, and contribute to the next task, transient product analysis. It is not possible to get transient product analysis accurately with the present instrumentation, but if it were it could lend great insight into the phenomena of functional group desorption which is essential for the formation of surface active sites.

APPENDIX A

HYDROGASIFICATION RATE CALCULATIONS

The method used to calculate hydrogasification rate of chars in this study involved 11 steps. Before an experiment, the char was weighed and calibration data collected. During a reaction, sample collections were timed and taken at discrete intervals. After the experiment, the rate was calculated by dividing the amount of methane collected at each sampling by the collection time. A plot of time vs. rate was drawn on graph paper, and manually integrated by counting the number of squares below the curve up to each individual data point. From this, percent carbon conversion and instant rate were calculated. The 11 steps are listed below, followed by an example.

1. Initial char weight was taken, then the initial weight of carbon in the char was determined by the following equation:

$$\text{Initial Wt. Carbon} = (\text{Initial Wt. Char})(\%\ \text{Carbon in Char})$$

2. A calibration was made to determine the area of a chart recorder peak for a known amount of methane. An electronic integrator reported the area under a peak in terms of counts (# cts. cal.).

3. The amount of methane present in the full calibration loop at STP was calculated by using the following equation:

$$\#\text{cc } CH_4 \text{ cal.} = (1.81 \text{ cc loop})(4.9\%\ CH_4)\left(\frac{273\ K}{295\ K}\right)\left(\frac{740\ \text{mmHg}}{760\ \text{mmHg}}\right)$$

$$\#\text{cc } CH_4 \text{ cal.} = 0.0799 \text{ cc } CH_4 \text{ (STP)}$$

4. The total amount of methane taken in one sample during the reaction was determined at STP once the calibration was made and the attenuations were set:

$$\#\text{cc } CH_4 \text{ (STP)} = \frac{(0.0799)(\#\text{ cts. sample})(\text{atten. sample})}{(\#\text{ cts. cal.})(\text{atten. cal.})}$$

5. The absolute rate was calculated by dividing the total amount of methane from a sample collection by the collection time and the initial weight of carbon in the sample:

$$\text{Absolute Rate} = \frac{[\#\text{ cc } CH_4 \text{ (STP)}]}{(\text{Coll. Time})(\text{Initial Wt. C})}$$

6. The time at which each sample collection was taken was recorded during the reaction. A plot of absolute rate vs. time was drawn on graph paper.

7. A curve was drawn through the data points. The squares under the curve were counted between the beginning of the reaction and a given data point, as a means of manually integrating the curve to determine the area under the curve that corresponds to the given data point.

8. The value of one square on the graph was determined by the chosen scale:

$$\text{Block Value} = \left(\frac{\text{amount of time}}{\text{unit length}}\right)\left(\frac{\text{Abs. Rate}}{\text{unit length}}\right)$$

9. The total amount of methane given off per unit weight of carbon in the char up to a particular data point was then determined by multiplying the number of blocks under the curve by the value of each block:

$$CH_4\text{/Unit Wt. Carbon} = (\text{Block Value})(\#\text{ Blocks})$$

10. This was converted to % carbon conversion by the following equation:

$$\%\text{ C Conv.} = \frac{(CH_4\text{/Unit Wt. C})(12.011\text{ gC/mol})(100\%)}{22{,}400\text{ cc/mol(STP)}}$$

11. Once the % carbon conversion was known for the different samples, the instant rate could be calculated from the absolute rate:

$$\text{Inst. Rate} = (100\%)(\text{Abs. Rate})/(100\% - \%\text{ Carbon Conv.})$$

An example of the values calculated in determining the instant rate as a function of % carbon conversion during hydrogasification is given on the following page. The example is of the base case coal char.

Table A.1: BASE CASE COAL CHAR HYDROGASIFICATION RATE DATA AND CALCULATIONS

Initial Wt. Carbon = (0.1965g Char)(74.72% Carbon)

Initial Wt. Carbon = 0.1468g

Counts Calibration = 160

Attenuation of calibration set at 8.

Sample Number	Time into Run (min)	Coll. Time	Atten.	Counts of Counts
1	5	1	32	75
2	20	1	32	294
3	37	1	32	173
4	52	1	32	127
5	72	1	16	173
6	82	1	16	154
7	103	1	8	266
8	119	1	8	259
9	135	1	8	217
10	153	1	8	216

Block Value = (5.0 min)(0.1cc CH_4/min·g C)

Block Value = 0.5 ccCH_4/g C

Sample Number	Abs.1 Rate	Blocks to Point	% Conv.	Inst.2 Rate
1	1.02	2	0.05	1.02
2	4.00	98	2.63	4.11
3	2.35	207	5.56	2.49
4	1.73	267	7.15	1.86
5	1.18	324	8.68	1.29
6	1.05	357	9.57	1.16
7	0.90	387	10.39	1.00
8	0.88	414	11.11	0.99
9	0.74	440	11.80	0.84
10	0.74	465	12.47	0.84

1. Units [=] cc CH^4/min·g Carbon Initial

2. Units [=] cc CH_4/min·g Carbon Instant

REFERENCES

1. Steinberg,M., in '**1987 International Conference on Coal Science**', (Eds J.A.Moulijn et al.), Elsevier Science Publishers B.V., Amsterdam, **11**, 953 (1983).

2. Hirsch,R.L., J.E.Gallagher Jr., R.R.Lessard, and R.D.Wesselhoft, **Science, 215**, 121 (1982).

3. Mims,C.A., and J.J.Krajewski, **J. Catal., 102**, 140 (1986).

4. Blackwood,J.D., **Aust. J. Applied Sci.**, 199 (1962).

5. Blackwood,J.D. and D.J.McCarthy, **Aust. J. Chem.**, **19**, 797 (1966).

6. Blackwood,J.D., **Aust. J. Chem.**, **15**, 397 (1962).

7. Blackwood,J.D., **Aust. J. Chem.**, **12**, 14 (1959).

8. Blackwood,J.D., D.J.McCarthy, and B.D.Cullis, **Aust. J. Chem.**, **20**, 2525 (1967).

9. Blackwood,J.D., B.D.Cullis, and D.J.McCarthy, **Aust. J. Chem.**, **20**, 1561 (1967).

10. Makino,M. and Y.Toda, **Fuel, 60**, 321 (1981).

11. Cao,J.-R. and M.H.Back, **Carbon, 20**, 505 (1982).

12. Juntgen,H., **Carbon, 19**, 167 (1981).

13. Lizzio,A.A., H.Jiang, and L.R.Radovic, **Carbon, 28**, 7 (1990).

14. Huttinger,K.J. and J.S.Nill, **Carbon, 28**, 457 (1990).

15. Tomita,A., O.P.Mahajan, and P.L.Walker Jr., **Fuel, 56**, 137 (1977).

16. Zielke,C.W. and E.Gorin, **Ind. and Eng. Chem., 47**#4, 820 (1955).

17. Otto,K. and M.Shelf, **Chem. Eng. Commun., 5**, 223 (1980).

18. Freund,H. **Fuel, 64**, 657 (1985).

19. Walker,P.L.Jr., **Carbon, 24**#4, 379 (1986).

20. Adams,K.E., D.R.Glasson, and S.A.A.Jayawerra, **Carbon, 27**, 95 (1989).

21. Radovic,L.R., P.L.Walker, and R.G.Jenkins, **Fuel, 62**, 849 (1983).

22. DeKoranyi,A., **Carbon, 27**, 55 (1989).

23. Tong,S.B., P.Pareja, and M.H.Back, **Carbon, 20**#3, 191 (1982).

24. Cypres,R., D.Planchon, and C.Braekman-Danhuex, **Fuel, 64**, 1375 (1985).

25. Blackwood,J.D. and D.J.McCarthy, **Aust. J. Chem., 20**, 2003 (1967).

26. Feldkirchner,H.L. and H.R.Linden, **I&EC Process Design and Development**, **2**#2, 153 (1963).

27. Wood,B.J. and K.M.Sancier, **Cata. Rev. Sci. Eng., 26**, 233 (1984).

28. Laine,N.R., F.J.Vastola, and P.L.Walker Jr., **J. of Phys. Chem., 67**, 2030 (1963).

29. Yang,R.T. and R.Z.Duan, **Carbon, 23**#3, 325 (1985).

30. Pan,Z.J. and R.T.Yang, **J. Catal., 123**, 206 (1990).

31. McKee,D.W. in **'Chemistry and Physics of Carbon'**, (Eds P.L.Walker Jr. and P.A.Thrower), Marcel Dekker, New York, **16**#1 (1981).

32. Yang,R.T. and K.L.Yang, **Carbon, 23**#5, p.537 (1985).

33. Cao,J.R and M.H.Back, **Carbon, 30**#6, 505 (1981).

34. Shaw,J.T., **Proc. Intern. Conf. Coal Science**, 209 (1981).

35. Gilberson,R.C. and J.P.Walker, **Carbon, 3**, 521 (1966).

36. Biderman,D.L., A.J.Miles, F.J.Vastola, and P.L.Walker Jr., **Carbon, 14**, 351 (1976).

37. Huttinger,K.J. **Fuel, 62**, 166 (1983).

38. Mims,C.A. and J.K.Pabst, **ACS Div. Fuel Chem. Prepr., 25**#3, 263 (1980).

39. Mims,C.A. and J.K.Pabst, **Fuel, 62**, 176 (1983).

40. Huttinger,K.J. and R.Minges, **Fuel, 65**, 1122 (1986).

41. McKee,D.W. and D.Chatterji, **12th Biennial Conference on Carbon**, Pittsburg, PA, 189-191 (1975).

42. Huttinger,K.J. **ACS Div. Fuel Chem. Prepr., 34**#1, 56 (1989).

43. Carangelo,R.M., P.R.Solomon, and D.J.Gerson, **Fuel, 66**, 960 (1987).

44. Hauge,R.H., L.Fredin, J.Chu, and J.L.Margrave, **ACS Div. Fuel Chem., 28**#1, 35 (1983).

45. Walker,P.L.Jr., **Carbon, 28**, 261 (1990).

46. Phillips,R.F., F.J.Vastola, and P.L.Walker Jr., **Carbon, 8**, 197 (1970).

47. Hart,P.J., F.J.Vastola, and P.L.Walker Jr., **Carbon, 5**, 363 (1967).

48. Treptau,M.H. and D.J.Miller, **Carbon, 29**, 531 (1991).

49. Toomajian,M., M.Lussier, and D.J.Miller, **ACS Div. Fuel Chem. Prepr., 36**#1, 139 (1991).

50. H.Zoheidi and D.J.Miller, **Carbon, 25**, 809 (1987).

51. Ergun,S., **J. Phys. Chem., 60**, 480 (1956).

52. Saber,M.J., J.L.Falconer, and L.F.Brown, **Fuel, 65**, 1356 (1986).

53. Hashimoto,K., K.Miura, J.J.Xu, and A.Watanabe, **Chem. Lett., 5**, 555 (1984).

54. Muhlen,H.-J., K.H.vanHeek, and H.Juntgen, **Fuel, 65,** 591 (1986).

55. Tromp,P.J.J., F.Kapteijn, J.J.Boon, and J.A.Moulijn, **Int'l Conf. on Coal Sci.**, 537 (1987).

56. Keleman,S.R. and H.Freund, **ACS Div. Fuel Chem. Prepr.**, **32#1**, 318 (1987).

57. Treptau,M.H. and D.J.Miller, **ACS Div. Fuel Chem. Prepr.**, **34#1**, 176 (1989).

58. Zoheidi,H. and D.J.Miller, **Carbon, 25**, 256 (1987).

59. Noh,J.S. and J.A.Schwarz, **Carbon, 28**, 675 (1990).

60. Ohtsuka,Y., K.Itagaki, K.Higashiyama, A.Tomita, and Y.Tamai, **Neaoyo Kyokaishi, 60**, 437 (1981).

61. Harbour,J.R., M.J.Walzak, W.Limburg and J.Yanus, **Carbon, 24#6**, 725 (1986).

62. Papirer,E., S.Li, and J.-B.Donnett, **Carbon, 25**, 243 (1987).

63. Cao,J.R. and M.H.Back, **Carbon, 23#2**, 141 (1985).

64. Bohem,H.P., E.Diehl, W.Heck, and R.Sappok, **Angew. Chem. Inter. Edit.**, **3#10**, 669, (1964).

65. Voll,M. and H.P.Bohem, **Carbon, 9**, 481 (1971).

66. Blackwood,J.D. **Carbon, 12**, 14 (1959).

67. Studebaker,M.L. and R.W.Rinehart Sr., **Rubb. Chem. Tech., 45**, 106 (1972).

68. Garten,V.A., D.E.Weiss, and J.B.Willis, **Aust. J. Chem., 10**, 309 (1957).

69. Barton,S.S. and B.H.Harrison, **Carbon, 13**, 283 (1975).

70. Barton,S.S., D.Gillespie, and B.H.Harrison, **Carbon, 11**, 649 (1973).

71. Barton,S.S., G.L.Boulton, and H.Harrison, **Carbon, 10**, 395 (1972).

72. Puri,B.R., D.D.Singh, J.Nath, and L.R.Sharma, **Ind. Eng. Chem., 50**, 1071 (1958).

73. Puri,B.R. and R.C.Banasal, **Carbon, 1,** 457 (1964).

74. Kolthoff,I.M. **J. Am. Chem. Soc., 54,** 69 (1932).

75. Nemerovets,N.N., V.F.Surovikin, S.V.Orekhov, G.V.Sazhin, and N.G.Sadovnichuk, **Solid Fuel Chem. (Russian), 14#4,** 120 (1980).

76. Sellitti,C., J.L.Koenig, and H.Ishida, **Carbon, 28,** 221 (1990).

77. King,A., **J. Chem. Soc.,** 1489 (1937).

78. Garten,V.A. and D.E.Weiss, **Aust. J. Chem., 8,** 68 (1955).

79. Miura,K., M.Makino, and P.L.Silveston, **Fuel, 69,** 580 (1990).

80. Dollimore,J., C.M.Freedman, B.H.Harrison, and D.F.Quinn, **Carbon, 8,** 587 (1970).

81. Tomita,A. and Y.Tamai, **J. Catal., 27,** 293 (1972).

82. Tomita,A. and Y.Tamai, **J. Phys. Chem.,** 78, 2254 (1974).

83. Tomita,A., N.Sato, and Y.Tamai, **Carbon, 12,** 143 (1974).

84. McKee,D.W., **Carbon, 12,** 453 (1974).

85. Nahas,N.C., **Fuel, 62,** 239, (1983).

86. Kubiak,H., H.J.Schroter, A.Sulimma, and K.H.vanHeek, **Fuel, 62,** 242 (1983).

87. Baker,R.T.K., R.D.Sherwood, and E.G.Derouane, **J. Catal., 75,** 382 (1982).

88. Nishiyama,Y., T.Haga, O.Tamura, and N.Sonehara, **Carbon, 28#1,** 185 (1990).

89. Huttinger,K.J. and P.Schleicher, **Fuel, 60,** 1005 (1981).

90. Baker,R.T.K. and J.J.Chludzinski Jr., **Carbon, 19,** 75 (1981).

91. Gothel,P.J. and R.T.Yang, **J. Catal.,** 101, 342 (1986).

92. Holstein,W.L. and M.Boudart, **J. Catal., 72**, 328 (1981).

93. Zoheidi,H., **Ph.D. Dissertation**, Michigan State University, East Lansing, MI (1987).

94. Lang,R.J. and R.C.Neavel, **Fuel, 61**, 620 (1982).

95. McKee,D.W. and D.Chatterji, **Carbon, 13**, 381 (1975).

96. McKee,D.W. and D.Chatterji, **Carbon, 16**, 53 (1978).

97. McKee,D.W., C.L.Spiro, P.G.Koski, and E.L.Lamby, **Fuel, 62**, 218 (1983).

98. Veraa,M.J. and A.T.Bell, **Fuel, 57**, 194 (1978).

99. Wood,J.B., R.H.Fleming, and H.Wise, **J. Am. Chem. Soc., 63**, 1600 (1984).

100. Wood,J.B., R.D.Brittain, and K.H.Lau, **Carbon, 23**, 73 (1985).

101. Long,F.J. and K.W.Sykes, **J. Chem. Phys., 47**, 361 (1950).

102. Wen,W.Y., **Cata. Rev. Sci. Eng., 22**, 1 (1980).

103. Sams,D.A., T.Talverdian, and F.Shadman, **Fuel, 64**, 1208 (1985).

104. Mims,C.A. and J.K.Pabst, **Proc. Int. Conf. on Coal Science**, Verlag Gluckauf GmbH, Essen, 730-736 (1981).

105. Mims,C.A., K.D.Rose, M.T.Melchior, and J.K.Pabst, **J. Am. Chem Soc., 104**, 6886 (1982).

106. Yuh,S.J. and E.E.Wolf, **J. Am. Chem. Soc., 63**, 1604 (1984).

107. Saber,J.M., J.L.Falconer, and L.F.Brown, **J. Catal., 90**, 23 (1984).

108. Wood,R.E. and G.R.Hill, **ACS Div. Fuel Chem. Prepr., 17**, 1 (1972).

109. Gardner,N., E.Samuels, and K.Wilkes, **Adv. Chem. Ser., 131**, 217 (1974).

110. Matsumoto,S. and P.L.Walker Jr., **Carbon, 27**, 395 (1989).

111. Formella,K., P.Leonhardt, A.Sulimma, K.H.vanHeek, and H.Juntgen, **Fuel**, **65**, 1471 (1986).

112. Bruno,G., L.Cavvani, and G.Passoni, **Fuel**, **65**, 1473 (1986).

113. Toomajian,M.E., **Masters Thesis**, Michigan State University, East Lansing, MI (1991).

114. Bishop,M. and D.L.Ward, **Fuel**, **37**, 191 (1958).

115. Benedict,M.A., Michigan State University, (1991).

116. Commercial Testing and Engineering Co., Lombard, IL (1990).